FINITE ELEMENT MODELLING OF INNOVATIVE CONCRETE-FILLED TUBULAR COLUMNS UNDER ROOM AND ELEVATED TEMPERATURES

European Project FRISCC

“Fire Resistance of Innovative and Slender Concrete Filled Tubular Composite Columns”

FINITE ELEMENT MODELLING OF INNOVATIVE CONCRETE-FILLED TUBULAR COLUMNS UNDER ROOM AND ELEVATED TEMPERATURES

European Project FRISCC
"Fire Resistance of Innovative and Slender Concrete Filled Tubular Composite Columns"

Project carried out with a financial grant of the Research Programme of the Research Fund for Coal and Steel (RFSR-CT_2012_00025)

The contents of this publication have been reviewed by the Editorial Board of the UPV through the peer review process.

First edition, 2013

http://www.lalibreria.upv.es/ Ref.: 6143

ISBN: 978-84-9048-123-3 (printed version)

CONTENTS

Foreword

Concrete-filled steel tubular (CFST) members are commonly used as composite columns in modern buildings. However, the current guidelines for member design in fire (EN1994-1-2) have been proved to be unsafe once the relative slenderness is higher than 0.5. In addition, the simplified design methods of Eurocode 4 are limited to circular or square CFST columns, while in practice columns with rectangular and elliptical hollow sections are being increasingly used because of their architectural aesthetics.

The main objective of the Project FRISCC (Fire Resistance of Innovative and Slender Concrete Filled Tubular Composite Columns) funded by the European Union with the contract RFSR-CT_2012_00025 is to develop a safe methodology for the fire design of slender concrete-filled tubular columns and additionally to extend it to innovative composite sections (CFST with elliptical cross-section and with embedded steel core).

The project is divided into several parts: evaluation of the existing design methods, experimental tests, numerical simulations, simplified design methods, design tools, dissemination and code additions and coordination. This publication is in the framework of the numerical simulation work package.

The numerical modelling of CFST columns exposed to fire involves the use of material models at elevated temperatures. The more common procedure for analysing the fire behaviour of such members is to conduct a heat transfer analysis for computing the temperature field and afterwards a stress/deformation analysis for calculating the structural response. Nodal temperatures are stored as a function of time in the heat transfer analysis results and then read into the stress analysis as a predefined field. Therefore, this is a task which requires advanced knowledge in finite element modelling.

The validation of nonlinear numerical models is necessary to demonstrate that these models are capable of accurately reproducing the observed physical behaviour, in such a way that they can be used to conduct parametric studies to generate further results. These results will enable a wider range of parameters to be considered than it is possible in the physical tests, and will form the basis for the development of design recommendations.

Several technical committees, as the EG EN 1993-1-2 and EG EN 1994-1-2, have expressed their doubts about which parameters have to be considered in a nonlinear finite element analysis. For instance, the possibility to include geometrical imperfections in advanced design methods by a sinusoidal initial bow imperfection is being questioned. Also, the results of other RFCS projects from EU show that is necessary to take into account residual stresses in advanced methods, as they have a certain influence combined with the member slenderness and steel grade.

The partners of the project FRISCC considered important to organize a workshop in which they could discuss and clarify all the issues related to the numerical simulation of CFST columns under fire. The workshop "**Numerical modelling of the fire resistance of concrete-filled tubular columns**" was held in Hannover (Germany) on the 19th of February 2013, and was attended by the different partners of the Project involved in numerical modelling: Universitat Politècnica de València (UPV), Gottfried Wilhelm Leibniz Universität Hannover (LUH), Universidade de Coimbra, Centre Technique Industriel de la Construction Métallique (CTICM) and Imperial College London.

This publication is a compendium of the results presented by the different partners at the workshop, and tries to enlighten which are the parameters to take into account in the numerical modelling of this typology of structures and which are their suitable values, at the same time that gives recommendations on modelling techniques. The document is organized in the form of technical sheets, each of them focusing on a different aspect of the numerical modelling of this type of composite columns.

Dr. Manuel L. Romero

TECHNICAL SHEET 1

FINITE ELEMENT ANALYSIS OF THE FIRE BEHAVIOUR OF CONCRETE FILLED CIRCULAR HOLLOW SECTION COLUMNS

A. Espinós, M.L. Romero and A. Hospitaler

(Universitat Politècnica de València, Spain)

FINITE ELEMENT ANALYSIS OF THE FIRE BEHAVIOUR OF CONCRETE FILLED CIRCULAR HOLLOW SECTION COLUMNS

In this work, a nonlinear three-dimensional finite element model for evaluating the fire resistance of axially loaded CFT columns of circular cross-section is presented. Based on the results of a comprehensive sensitivity analysis, the values of the relevant parameters of the model are selected. The numerical model is validated against experimental fire tests, producing accurate predictions of the thermal and mechanical response of the columns. This numerical model is valid for evaluating the fire resistance of unprotected CFT columns filled with normal strength concrete and subjected to concentric axial loads.

1. INTRODUCTION

The use of concrete filled tubular (CFT) columns has increased in recent decades due to their excellent structural performance, which takes advantage of the combined effect of steel and concrete working together.

In the fire situation, the degradation of the material properties gives rise to an extremely nonlinear behaviour of these composite columns, which makes it difficult to predict their failure. Up until now, a large number of numerical models have been developed worldwide (Zha 2003, Renaud et al. 2003, Ding & Wang 2008, Hong & Varma 2009, Schaumann et al. 2009), which have helped to gain insight into the fire behaviour of this type of composite columns.

In this work, a nonlinear three-dimensional finite element model for evaluating the fire resistance of axially loaded concrete filled circular hollow section (CFCHS) columns is presented, which allows for a realistic representation of the fire behaviour of these types of composite columns. Based on the results of a comprehensive sensitivity analysis, the values of the relevant parameters of the model are selected.

The numerical model is validated by comparing its results with experimental fire tests of circular CFT columns available in the literature (Chabot & Lie 1992, Lie & Chabot 1992) as well as against the results of a series of fire tests carried out by the authors (Romero et al. 2011).

2. CHARACTERISTICS OF THE NUMERICAL MODEL

A three-dimensional numerical model for simulating the fire behaviour of concrete filled circular steel hollow section columns was developed with the aid of the general purpose nonlinear finite element analysis package ABAQUS (2010). The model consisted of three parts: the concrete core, the steel tube and the loading plate.

The model was meshed with three-dimensional eight-noded solid elements for both the steel tube and the concrete core, and two-noded truss elements for the reinforcing bars. The loading plate was meshed by means of four-noded solid elements. Based on the results of a mesh sensitivity study, a maximum finite element size of 2 cm was used. Fig. 1 shows the finite element mesh for one of the CFT column specimens analysed.

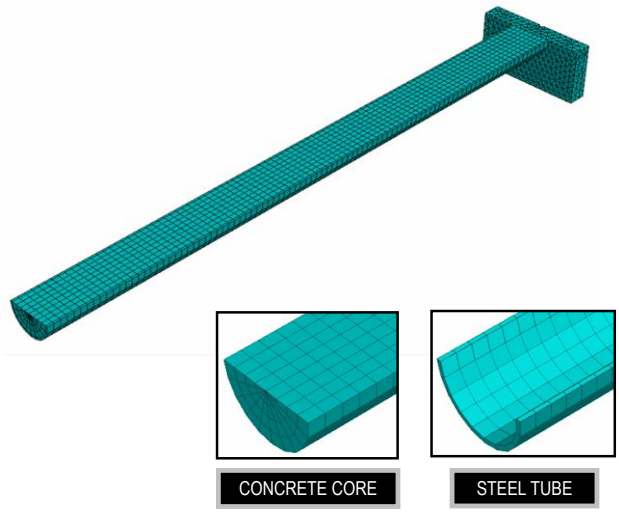

Fig. 1. Finite element mesh of the model.

The temperature dependent thermal and mechanical properties of the materials were accounted for in the numerical model. All the selected values will be further discussed in the sensitivity analysis section.

The thermal properties for concrete at elevated temperatures were extracted from EN 1992-1-2 (CEN 2004). The moisture content of the concrete infill was taken into account through a peak value in the specific heat, representing the latent heat of water vaporisation. For structural steel, the temperature dependent thermal properties recommended in EN 1993-1-2 (CEN 2005) were adopted. The value of the thermal expansion coefficient for concrete recommended by Hong & Varma (2009) was employed: $\alpha_c = 6\times10^{-6}$ $^{o}C^{-1}$.

For characterizing the mechanical behaviour of concrete, the Drucker-Prager model was selected. The stress-strain relations for concrete under compression proposed by Lie (1984) were employed. The initial elastic behaviour was defined at each temperature by means of the elastic modulus and Poisson's ratio. The Poisson's ratio was assumed to be independent of the temperature, and equal to 0.2.

For representing the mechanical behaviour of steel, an isotropic elasto-plastic model with the von Mises yield criterion was used. The constitutive model selected for representing the uniaxial behaviour of steel at elevated temperatures was that from EN 1993-1-2 (CEN 2005). The Poisson's ratio was assumed to be independent of the temperature, and equal to 0.3.

The numerical model took into account the initial geometric imperfection of the columns, which was obtained as the first buckling mode shape of the hinged column multiplied by an amplification factor. For this purpose, a previous eigenvalue analysis was conducted over a pinned-pinned column. Once the initial shape of the column was obtained, it was imported to the mechanical model as the starting geometry from which to run the analysis. An amplification factor of $L/1000$ was used.

A sequentially coupled thermal-stress analysis was designed. The analysis was performed by first conducting a pure heat transfer analysis for computing the temperature field and afterwards a stress/deformation analysis for calculating the structural response. Nodal temperatures were stored as a function of time in the heat transfer analysis results and then read into the stress analysis as a predefined field.

The thermal resistance at the boundary between the steel tube and the concrete core was taken into account in the numerical model. Through the results of a sensitivity analysis, which will be presented later on in Section 4, it was decided to assume a constant value of 200 W/m^{2}K for the gap conductance at the boundary between the steel tube and the concrete core.

3. VALIDATION OF THE MODEL

The numerical model was on a first stage validated by comparing its results with experimental fire tests of circular CFT columns available in the literature, from the National Research Council of Canada (Chabot & Lie 1992, Lie & Chabot 1992).

A first validation step consisted of comparing the evolution of temperature along the fire exposure time in the numerical simulations with the temperatures recorded in the tests at those sectional points where thermocouples were installed. The comparison between measured and calculated temperatures is shown in Fig. 2 for one of the column specimens studied.

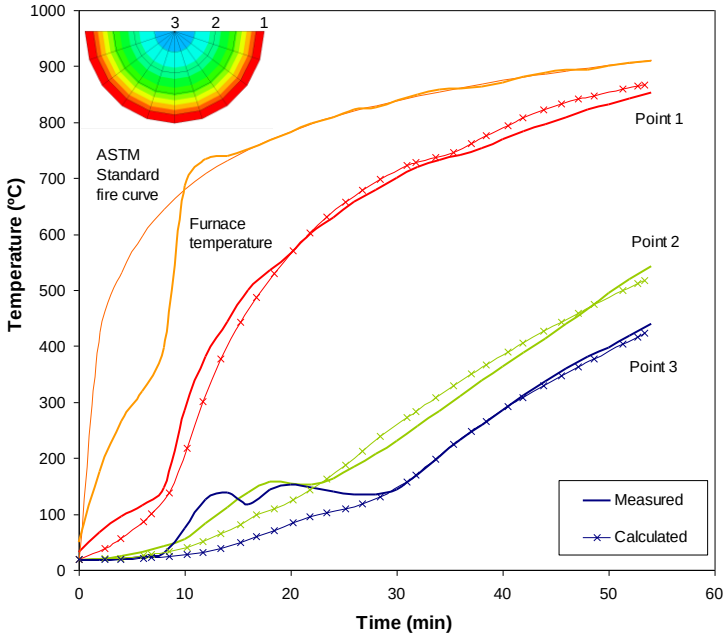

Fig. 2. Comparison between measured and predicted temperatures for column C-02.

As can be seen, the overall temperature-time response in the selected points followed accurately the test results, with the exception of the range of temperatures between 100 and 200 ºC in the concrete layers, where the evaporation of moisture occurs.

For each of the columns analysed, the axial displacement at the top end of the column versus the fire exposure time was registered during the simulation, comparing this curve with the one obtained in the fire test. Fig. 3 shows the comparison between both curves for one of the column specimens studied.

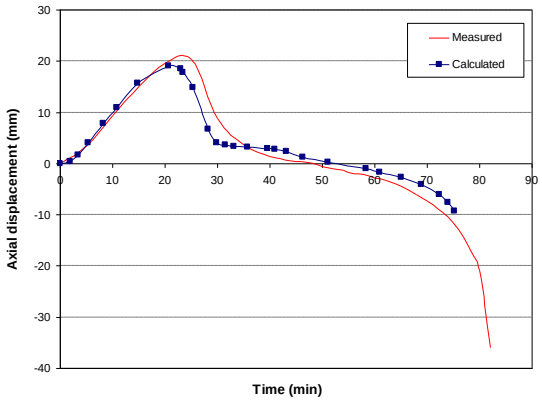

Fig. 3. Comparison of measured and predicted axial displacement, column C-17.

Fig. 4 shows the comparison between the numerical predictions and test results, in terms of fire resistance rating (FRR). The agreement with the experiments was considered acceptable given the uncertainties in some of the test data, with a good average value of the error (1.07 mean value) and a moderated dispersion of results (0.18 standard deviation).

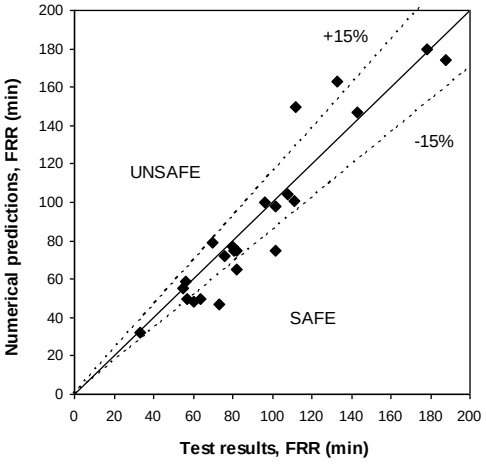

Fig. 4. Comparison of FRR between the numerical predictions and the test results (Canadian tests).

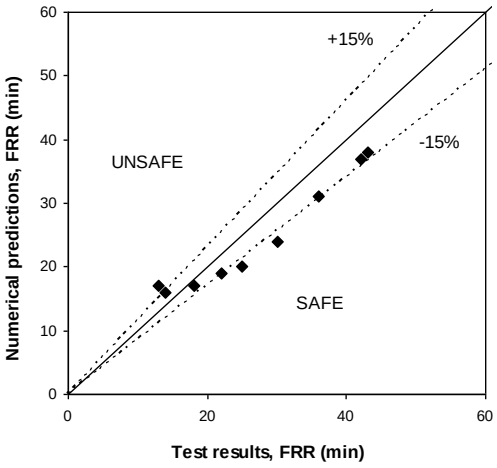

Fig. 5. Comparison of FRR between the numerical predictions and the test results (own tests).

On a second stage, the numerical model was validated against a series of fire tests carried out by the authors. The experiments were performed in the testing facilities of AIDICO (Instituto Tecnológico de la Construcción) in Valencia, Spain. In this experimental program, sixteen fire tests were carried out on normal and high strength concrete filled tubular columns of circular section. Plain, bar-reinforced and steel fiber reinforced concrete was used as infill. The details of this experimental program can be found in Romero et al. (2011). For this series of tests, an average error of 1.09 and a standard deviation of 0.16 in the FRR prediction were obtained (Fig. 5), similar to those values obtained in the comparison with the Canadian tests, which confirms that the numerical model is sufficiently validated against different sources and capable for predicting the fire response of normal strength CFCHS columns.

4. SENSITIVITY ANALYSIS

An extensive sensitivity analysis was carried out in order to study the influence of the main parameters of the model and to find their suitable values. Specimen C-05 from the Canadian tests (Lie & Chabot 1992) was selected for carrying out this study.

4.1. STEEL-CONCRETE INTERFACE FRICTION MODEL

Three options were studied for the steel-concrete frictional interaction: the first option used the classical Coulomb friction model with a friction coefficient equal to 0.3, the second option assumed a full slip between the steel tube and the concrete core (frictionless contact) and the third option considered the existence of a full bond at the steel-concrete interface (rough contact).

The full bond model deviated excessively from the real behaviour of the column, as it can be seen in Fig. 6. In turn, the Coulomb friction model and full slip model produced exactly the same results, being both close to the measured curve, therefore it can be confirmed that a full slip occurs at the steel-concrete interface in the fire situation, since the different thermal expansions cause the separation of the steel tube from the concrete core at elevated temperatures.

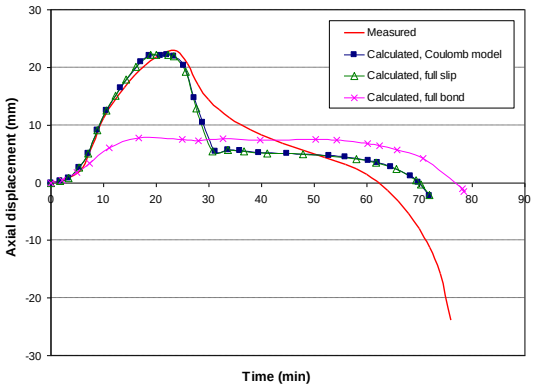

Fig. 6. Comparison of measured and predicted axial displacement with different friction models.

4.2. GAP THERMAL CONDUCTANCE

In a first approach, a constant value of 200 W/m^{2}K for the gap conductance was employed, as recommended by Ding & Wang (2008). In a second approach, the interfacial thermal conductance was expressed as a function of temperature as suggested by Ghojel (2004). The third approach considered the existence of a perfect thermal contact at the steel-concrete interface, that is, the temperature at the contacting surfaces of steel and concrete is the same.

As it can be seen in Fig. 7, the model proposed by Ghojel produced the best estimations in terms of failure time, although adopting a constant value of 200 W/m^{2}K produced acceptable results as well, which in this case remain on the safe side. Assuming that no thermal resistance exists at the steel-concrete interface (perfect contact) is not so realistic and leads to very conservative estimations, since it predicts a faster temperature rise.

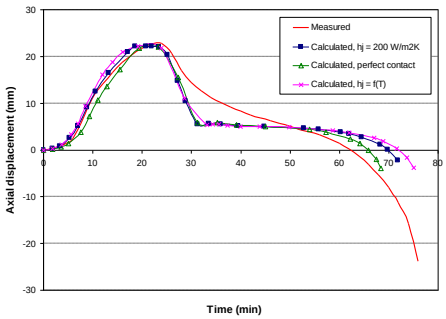

Fig. 7. Comparison of measured and predicted axial displacement with different gap conductance values.

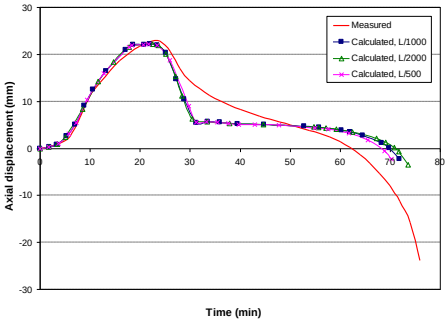

Fig. 8. Comparison of measured and predicted axial displacement with different initial imperfections.

4.3. INITIAL GEOMETRIC IMPERFECTION

In order to represent the initial geometric imperfection of the columns, the deformed shape of the first buckling mode of a hinged column was obtained, and afterwards amplified by means of an imperfection factor for each of the geometries under study.

Different values for the out-of-straightness of the column ranging from $L/500$ to $L/2000$ were studied, producing the results shown in Fig. 8. From this study, it can be recommended that values no higher than $L/500$ are adopted, being optimum to employ an amplitude of $L/1000$ – $L/2000$, as normally assumed by researchers (Ding & Wang 2008, Hong & Varma 2009).

4.4. MATERIAL MODELS AT ELEVATED TEMPERATURES

Steel

For steel, three models were studied and compared: EN 1993-1-2 (CEN 2005), Lie (1984) and Yin et al. (2006). EN 1993-1-2 model produced the more accurate response, whereas the model from Lie predicted an excessively resistant behaviour, as it can be seen in Fig. 9. The model from Yin did not produce a converged solution. According to these results, the model from EN 1993-1-2 was selected for defining the mechanical behaviour of steel at elevated temperatures.

Two options were studied for modelling the thermal expansion of steel at elevated temperatures. On one hand, the temperature dependent values of the thermal expansion coefficient from EN 1993-1-2 (CEN 2005) were studied. On the other hand, the constant value recommended by Hong & Varma (2009), $\alpha_s = 12\times10^{-6}$ $^oC^{-1}$, was used. The EN 1993-1-2 thermal expansion model produced very accurate results, whereas the constant value proposed by Hong & Varma predicted a shorter maximum axial displacement, as shown in Fig. 10. The temperature dependent formulation from EN 1993-1-2 was therefore selected.

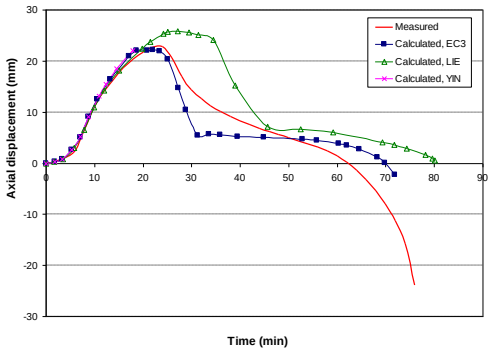

Fig. 9. Comparison of measured and predicted axial displacement with different steel models.

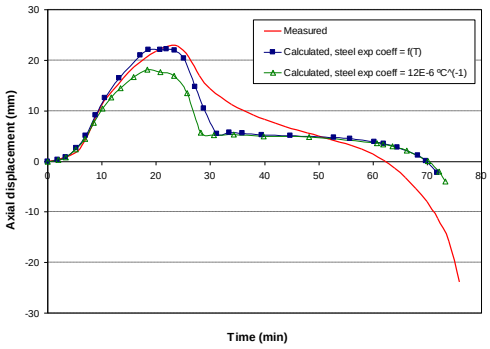

Fig. 10. Comparison of measured and predicted axial displacement with different steel thermal expansion coefficients.

Concrete

In the case of concrete, a variety of constitutive models at elevated temperatures exists in the literature. Five of them were studied in this research: Lie (1984), EN 1992-1-2 (CEN 2004), Anderberg & Thelandersson (1976), Li & Purkiss (2005) and Schneider (1988). Among all these models, the model from Lie was the one that best predicted the fire resistance of the columns, as it can be seen in Fig. 11. Regarding EN 1992-1-2 model, it produced the most conservative results, deviating from the real response of the columns. Therefore, the stress-strain relations proposed by Lie were used for defining the uniaxial behaviour of concrete at elevated temperatures in the numerical model.

Two options were studied for modelling the thermal expansion of concrete at elevated temperatures: the temperature dependent formulation from EN 1992-1-2 (CEN 2004) and the constant value recommended by Hong & Varma (2009), $\alpha_c = 6\times10^{-6}$ $^oC^{-1}$. This constant value produced remarkably better results for concrete, as shown in Fig. 12, while the model form EN 1992-1-2 resulted in a very unrealistic response, giving place to an excessive axial displacement in the stage when the concrete core is sustaining the majority of the applied load.

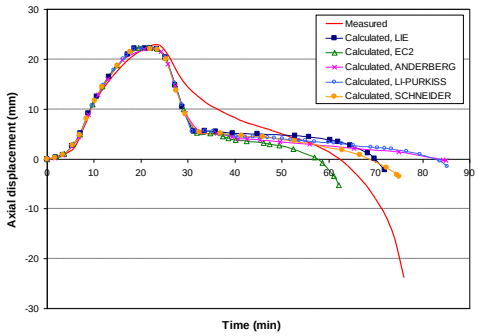

Fig. 11. Comparison of measured and predicted axial displacement with different concrete models.

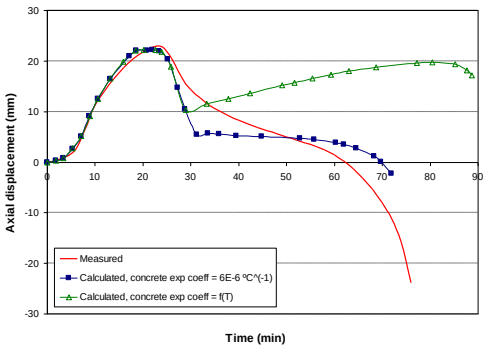

Fig. 12. Comparison of measured and predicted axial displacement with different concrete thermal expansion coefficients.

5. SUMMARY AND CONCLUSIONS

In this work, the fire behaviour of axially loaded concrete filled steel tubular columns of circular cross-section was investigated through a three-dimensional finite element model. The accuracy of the numerical model was verified by means of test results available in the literature as well as against own tests, showing that it can provide a realistic representation of the fire response of normal strength CFCHS columns. Good agreement with the tests was obtained in the prediction of the thermal and mechanical response of the columns.

By means of the validated numerical model, a comprehensive sensitivity analysis was carried out, from which a number of modelling recommendations were obtained.

For modelling the tangent behaviour at the steel-concrete interface, a full slip can be assumed and thus a frictionless contact model adopted, since in the fire situation the different thermal expansions cause the transverse separation of the steel tube from the concrete core.

Regarding the gap thermal conductance at the steel-concrete interface, the model proposed by Ghojel (2004) produces the best estimations in failure time, although adopting a constant value of 200 W/m^2K is more simplistic and produces acceptable results as well.

It is recommended to employ an amplitude value of $L/1000 - L/2000$ for the initial geometric imperfection of the columns.

For steel, the EN1993-1-2 constitutive model produces the most accurate response, while for concrete the model developed by Lie (1984) is the one that best predicts the mechanical behaviour in the fire situation.

The EN1993-1-2 thermal expansion model provides accurate results for steel, whereas for concrete the constant value $\alpha_c = 6\times10^{-6}\ ^oC^{-1}$ recommended by Hong & Varma (2009) produces the best results.

REFERENCES

ABAQUS. 2010. *ABAQUS/Standard Version 6.10 User's Manual: Volumes I-III*. Pawtucket, Rhode Island: Hibbitt, Karlsson & Sorensen, Inc.

Anderberg Y, Thelandersson S. 1976. *Stress and deformation characteristics of concrete, 2-experimental investigation and material behaviour model. Bulletin 54*. Lund, Sweden: Lund Institute of Technology.

CEN. 2004. *EN 1992-1-2, Eurocode 2: Design of concrete structures, Part 1.2: General rules – Structural fire design*. Brussels, Belgium: Comité Européen de Normalisation.

CEN. 2005. *EN 1993-1-2, Eurocode 3: Design of steel structures, Part 1.2: General rules – Structural fire design*. Brussels, Belgium: Comité Européen de Normalisation.

Chabot M, Lie TT. 1992. *Experimental studies on the fire resistance of hollow steel columns filled with bar-reinforced concrete*. Internal report No. 628. Ottawa, Canada: Institute for Research in Construction, National Research Council of Canada (NRCC).

Ding J, Wang YC. 2008. Realistic modelling of thermal and structural behaviour of unprotected concrete filled tubular columns in fire. *Journal of Constructional Steel Research* 64:1086-1102.

Espinos A. 2012. *Numerical analysis of the fire resistance of circular and elliptical slender concrete filled tubular columns*. Doctoral thesis. Valencia, Spain: Universitat Politècnica de València.

Ghojel J. 2004. Experimental and analytical technique for estimating interface thermal conductance in composite structural elements under simulated fire conditions. *Experimental Thermal and Fluid Science* 28:347-354.

Hong S, Varma AH. 2009. Analytical modeling of the standard fire behavior of loaded CFT columns. *Journal of Constructional Steel Research* 65:54-69.

Li LY, Purkiss J. 2005. Stress-strain constitutive equations of concrete material at elevated temperatures. *Fire Safety Journal* 40(7):669-686.

Lie TT, Chabot M. 1992. *Experimental studies on the fire resistance of hollow steel columns filled with plain concrete*. Internal report No. 611. Ottawa, Canada: Institute for Research in Construction, National Research Council of Canada (NRCC).

Lie TT. 1984. A procedure to calculate fire resistance of structural members. *Fire and materials* 8(1):40-48.

Renaud C, Aribert JM, Zhao B. 2003. Advanced numerical model for the fire behaviour of composite columns with hollow steel section. *Steel and Composite Structures* 3(2):75-95.

Romero ML, Moliner V, Espinos A, Ibañez C, Hospitaler A. 2011. Fire behavior of axially loaded slender high strength concrete-filled tubular columns. *Journal of Constructional Steel Research* 67(12):1953-1965.

Schaumann P, Kodur V, Bahr O. 2009. Fire behaviour of hollow structural section steel columns filled with high strength concrete. *Journal of Constructional Steel Research* 65:1794-1802.

Schneider U. 1988. Concrete at high temperatures – A general review. *Fire Safety Journal* 13:55-68.

Yin J, Zha XX, Li LY. 2006. Fire resistance of axially loaded concrete filled steel tube columns. *Journal of Constructional Steel Research* 62(7):723-729.

Zha XX. 2003. FE analysis of fire resistance of concrete filled CHS columns. *Journal of Constructional Steel Research* 59:769-779.

TECHNICAL SHEET 2

3 D-MODELLING OF CONCRETE-FILLED CIRCULAR COMPOSITE COLUMNS WITH EMBEDDED STEEL CORE IN CASE OF FIRE

P. Schaumann and I. Kleiboemer

(Gottfried Wilhelm Leibniz Universität Hannover, Germany)

3 D-MODELLING OF CONCRETE-FILLED CIRCULAR COMPOSITE COLUMNS WITH EMBEDDED STEEL CORE IN CASE OF FIRE

The numerical simulation of composite columns at elevated temperature is covered by EN 1994-1-2. Nevertheless, there are a number of insufficiently investigated details using numerical models to design composite structures. In particular, the thermal and mechanical interface conditions between steel and concrete and the influence of residual stresses on the structural behaviour are uncertain. In this work, a 3 D numerical model of a composite column with embedded steel core in case of fire is presented. Detailed information is given concerning the applied material models and properties. Furthermore, the definition of both thermal and mechanical contact properties is described. A sub-model is introduced to transfer structural imperfections in terms of residual stresses resulting from a preliminary analysis to the main model. This technical sheet addresses details of the numerical model. Numerically determined fire resistances of various columns will be provided in future.

1. INTRODUCTION

Composite structures of steel and concrete take advantage of the material properties of both materials. Hence, it is possible to design very efficient and economic constructions. Composite columns are used in various structures such as stadiums, high-rise buildings or halls. Architects strive to design filigree structures, which led to the introduction of an innovative cross-section for composite columns. Those columns consist of a hollow steel section, a massive embedded steel core and concrete infill in between (see Fig. 1). This cross-section type comes along with a significantly increased load bearing capacity compared to other column types with identical outer dimensions. Hence, either higher loads can be applied or columns can be designed with smaller dimensions.

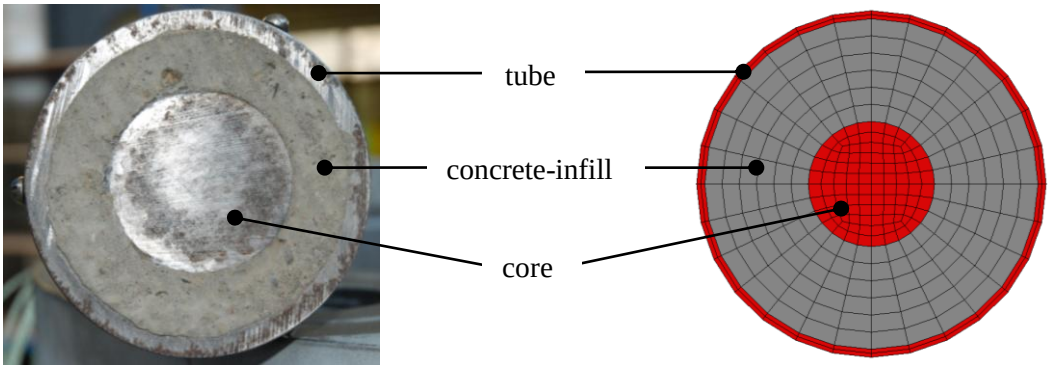

Fig. 1. Cross-section of concrete-filled column with embedded steel core.

Within the European research project FRISCC (Fire Resistance of Innovative and Slender Concrete Filled Tubular Composite Columns) various types of composite columns are studied. The particular subject investigated at Leibniz University Hannover

is the aforementioned innovative column type with embedded steel core. Predominantly, circular columns with massive, circular embedded steel cores are studied.

Aiming at an optimised cross-sectional design, it is necessary to perform investigations on the limited concrete cover between steel tube and core, which is accompanied by a reduced fire protecting effect. The verification of a sufficient bearing capacity both for ambient and elevated temperatures is needed for this innovative type of column.

The main research approach of this work is to investigate the influence of heat transfer conditions and residual stresses within the cross-section concerning the thermal and structural behaviour of composite columns. For this purpose, a 3 D model of a composite column with embedded steel core is presented.

2. DETAILS OF NUMERICAL SIMULATION

2.1. GENERAL

The scope of level 1 and level 2 design methods in EN 1994-1-2 (2010) does not include composite columns with massive steel cores yet. Hence, for the structural fire design of those columns it is just possible to perform either advanced calculation methods or fire tests. Due to the high costs of fire tests, it is recommended to perform numerical simulations instead. In doing so, it is possible to investigate a wide range of parameters. On the other hand, there is a number of insufficiently investigated items, which need to be defined using numerical models. The treatment of those items may lead to significantly different results whereas they are not standardised. In general, the main difficulties in simulating composite columns in case of fire are listed hereafter and visualised in Fig. 2.

(1) implementation of constitutive laws, especially for concrete
(2) modelling of the interface between concrete and steel
(3) reproduction of the actual boundary conditions
(4) modelling of the load introduction
(5) approximation of structural and geometrical imperfections

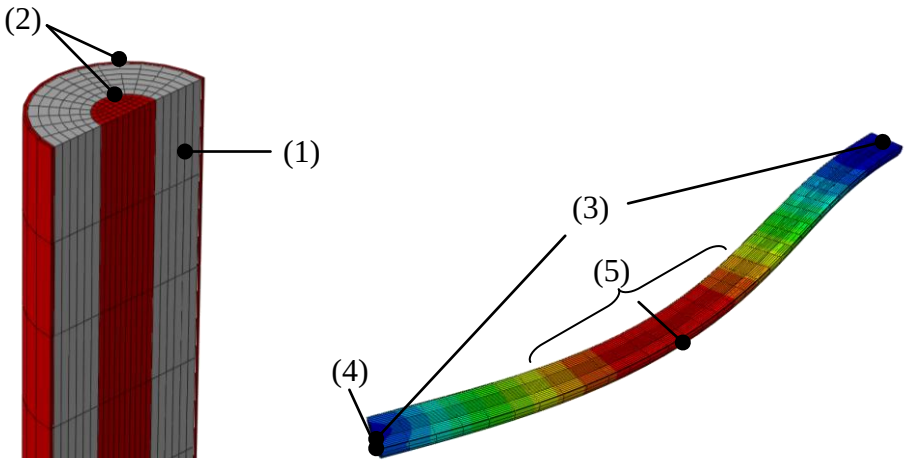

Fig. 2. Distinctive details for numerical simulations of composite columns.

For the analysis described hereafter, the software package Abaqus 10.1 (2010) is used. Accompanied with the Intel Fortran Compiler 10.1 it is furthermore possible to implement user-subroutines to Abaqus.

The column dimensions exemplarily used in the model described have already been used in practical applications. The outer diameter of the tube amounts to 193.7 mm with a thickness of 4.5 mm. The steel core has a diameter of 70 mm. Hence, the thickness of the concrete cover arises to 57.35 mm. As the numerical simulation is inspired by fire tests planned in the research project, the column length is chosen to 3.18 m according to the furnace length.

The investigated column has a symmetric cross-section, hence it is possible to reduce the model to a half-model. The half-model is still capable to reproduce all possible failure modes, whereas it has the advantage of a significantly reduced computing time.

Due to the introduction of residual stresses in the model (see section 0), a coupled thermal-mechanical analysis is performed instead of the commonly used sequentially coupled. Hence, the elements chosen are coupled temperature-displacement elements. They are labelled *C3D8T* meaning three-dimensional elements with eight nodes and an additional degree of freedom for temperature. Linear shape functions and full integration are applied.

The cross-section is discretised in 28 elements along the circumference and 64 along the column length (see Fig. 3).

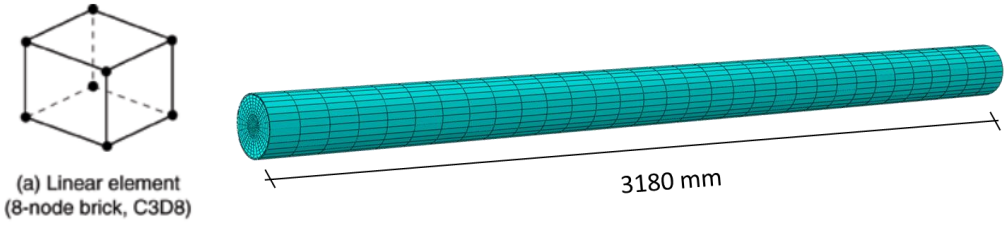

Fig. 3. Discretisation of composite column and visualisation of C3D8-element (Abaqus 2010).

The following paragraphs successively focus on the aforementioned details of modelling composite columns in case of fire.

2.2. MATERIAL PROPERTIES

Thermal analysis in Abaqus (2010) is based on the Fourier's equation. From equation (1) it is obvious that it is necessary to supply the parameters conductivity, density and specific heat to the program.

$$div\ \lambda\left(grad\ \theta\right)+Q=\rho c\frac{d\theta}{dt} \tag{1}$$

The specifications of EN 1994-1-2 are adopted concerning the temperature-dependent thermal material properties for steel and concrete. In accordance to DIN EN 1994-1-2/NA (2010), the upper limit of conductivity is utilised for concrete.

The peak value of the specific heat of concrete is dependent on the moisture content. Preliminary analysis showed that the assumption of 3 % moisture content leads to faster

heating of the column than 10 % moisture content. Hence, the assumption of 3 % is conservative and applied to the model.

Regarding the thermal elongation coefficient of steel and concrete again the definitions of EN 1994-1-2 (2010) are adopted. Other authors, e.g. Hong & Varma (2009), showed that the assumption of constant values amounting to $12 \cdot 10^{-6}$ K^{-1} and $6 \cdot 10^{-6}$ K^{-1} for steel and concrete respectively lead to quite similar results.

The simulation is performed with nominal values f_y = 355 MPa for both steel tube and core and f_c = 30 MPa for concrete, which corresponds to the material strengths proposed for the tests. The temperature-dependent decrease in material properties is adopted according to EN 1994-1-2 (2010). For both concrete and steel a temperature-dependent Poisson's ratio approximated from test results given in Ehm (1986) and Wohlfahrt (2001) is used (see Fig. 4).

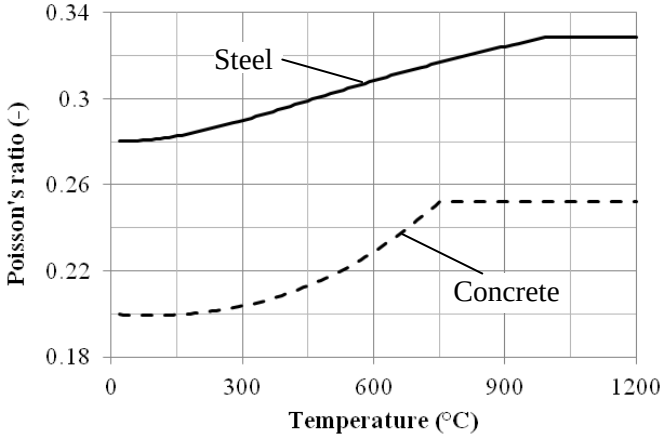

Fig. 4. Temperature-dependent Poisson's ratio.

There are several material models preset in Abaqus. For all material models it is necessary to define the σ-ε-relationship with true stresses and true strains. True stresses and true strains take into account the change in cross-sectional area in referring to the instantaneous area. Hence, the material values given in EN 1994-1-2 (2010) need to be transferred to true stresses and true strains before it is possible to adopt them in Abaqus (2010).

For the isotropic material steel, the definition of the stress-strain-curve is equal for compression and tension. The elastic branch is specified with the predefined material model *Elastic* based on Hooke's law. The plastic branch-definition occurs via the material model *Plastic*. Furthermore, isotropic hardening is considered.

To reproduce the σ-ε-relationship of concrete, the material model *Concrete Damaged Plasticity* is used for the plastic branch. This material model is based on the Drucker-Prager model and defines the 3 D-yield condition as a cone. For a realistic description of the yielding criterion a manipulation of the cone is possible via changing the eccentricity, the K-factor, the viscosity parameter and the dilation angle. The eccentricity smoothes the top of the cone and is defined temperature-dependent according to Grassl (2006). According to Lubliner (1989), which is the basis of this model, the K-factor is taken to 2/3. The viscosity parameter is taken to zero by default. Any shear deformation is accompanied by an enlargement and change in volume of the material. This is described via the dilation angle and depends on the grain shape and friction angle. For concrete the dilation angle is commonly taken to 30°, which is adopted in the model.

The material model is furthermore capable to consider the increase in compressive strength in multi-axial stress states. The ratio of biaxial compressive strength and un-damaged uniaxial compressive strength is defined with temperature-dependent values in the model. A damage formulation for tensions and for compression is still in process at the Institute for Steel Construction.

2.3. CONTACT PROPERTIES

The interface between concrete and steel needs to be defined regarding mechanical and thermal contact properties. In case of fire, the outer steel tube of concrete-filled tubular columns heats up faster and expands more than the concrete-infill. Hence, the load bearing capacity decreases rapidly due to the high temperature and can be omitted (for detailed investigations of the outer tube see also Schaumann et al. (2009)). Consequently, it is conservative to neglect the mechanical contact in this joint due to the poor mechanical properties.

Concerning the thermal contact property, the heat transfer is assumed to arise solely due to thermal conductance. Radiation and convection within gaps appearing during the analysis are neglected. Ideal conductance aims in conservative results, whereas a gap-dependent definition leads to more realistic temperatures. Another approach was introduced by Ding & Wang (2008), utilising a constant value of 200 W/m²K for the heat transfer coefficient during the whole analysis.

A sensitivity study was carried out to investigate the influence of the conduction coefficient. The resulting temperatures within the cross-section are compared for ideal heat transfer and the approach proposed by Ding & Wang (2008). The cross-section was heated by the ISO standard fire for 90 minutes. The results show significantly different temperatures reached in the middle of the core. The analysis using k = 200 W/m²K reaches 410 °C, whereas perfect heat transfer reaches 460 °C (see Fig. 5). The assumption of perfect heat transfer leads to higher temperatures, accompanied by a lower thermal gradient. The decrease in material properties due to higher temperatures is more decisive than the thermal gradient. Hence, an optimal heat transfer between concrete and steel is used for the analysis.

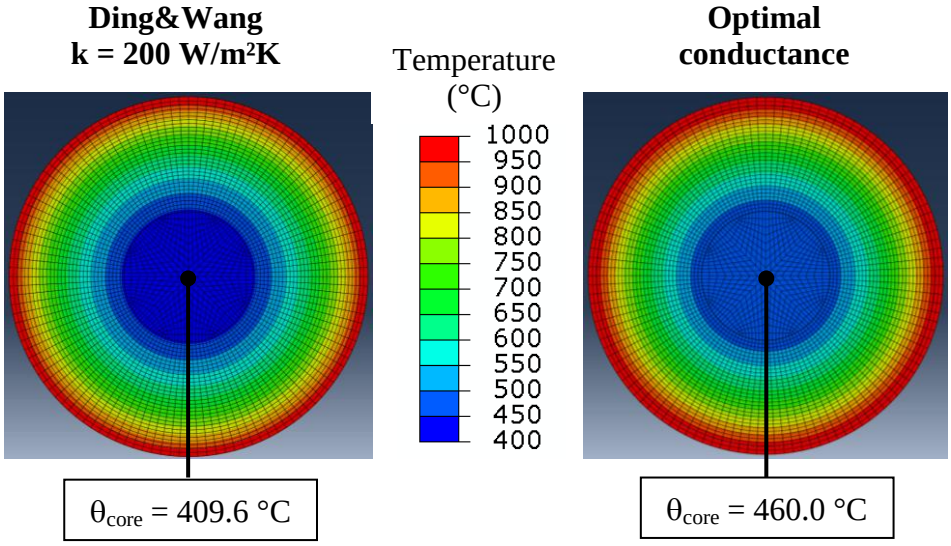

Fig. 5. Temperature distribution through cross-section for different thermal contact properties.

The cross-section investigated possesses a second joint between the concrete-infill and the steel core. Preliminary analysis showed that this joint does not separate during fire and hence mechanical contact is active. Both in normal and tangential direction contact properties need to be defined. In normal direction Hard contact is applied, transferring entire compressive forces but no tensile forces across the joint. The tangential behaviour is defined by Coulomb friction. Concerning the friction coefficient, various values have been used in models of composite columns, e.g. $\mu = 0.6$ (Hanswille 2008), $\mu = 0.6\text{-}0.8$ (Goralski 2006) or $\mu = 0.2\text{-}0.6$ (Johansson 2002). A temperature-dependent friction coefficient cannot be found in literature yet. None of those authors proposed data for the friction coefficient at elevated temperature. Within the research project, this parameter will be studied in detail, whereas up to now a constant value of $\mu = 0.6$ is adopted.

2.4. BOUNDARY CONDITIONS AND LOAD INTRODUCTION

The boundary conditions are chosen to represent a pinned-fixed column with free axial and tangential expansion. The model possesses a symmetry plane, leading to a significantly reduced computing time.

Immediate and concentrated forces may cause instabilities in numerical calculation. To avoid this, a loading plate is introduced on top of the column, which is loaded with uniform distributed compressive forces during a loading step. The loading plate is kept cold during the whole analysis. The interface between column and loading plate is defined by hard contact conditions.

2.5. IMPERFECTIONS

For consideration of geometrical imperfections, the first eigenmode of a preliminary buckle analysis is transferred to the model. The maximum amounting amplitude is scaled to 1/1000 of the column height.

Besides the aforementioned geometrical imperfections, structural imperfections are considered for the steel core as well. During the production process of massive steel cores residual stresses arise. Hamme & Schaumann (1987) showed that contrary to thin steel cross-sections, massive steel profiles come along with residual stresses, which cannot be neglected due to their remarkable amount. In various parts of the cross-section, those residual stresses may reach the yield strength.

There is no standardised approach to consider residual stresses in numerical simulations. Some rare approaches can be found in literature. Hanswille (2008) published a proposed stress distribution for massive circular steel profiles. In his approach, the amount of maximum tensile and maximum compressive stresses reach the same level. Compressive stresses develop in the outer regions, whereas in the inner area tensile stresses arise. In between, Hanswille (2008) proposes a quadratic stress distribution. The maximum amount of residual stresses varies with the diameter of the steel profile.

The cooling process was simulated in a secondary model in Abaqus (2010). The process was simulated starting at 1200 °C and finishing when temperatures drop under 100 °C in each element. The comparison of maximum and minimum residual stresses resulting from the simulation and the simplified approach by Hanswille (2008) is shown in Fig. 6. The results match well for most investigated diameters. The simplified approach by Hanswille (2008) is able to predict the maximum and minimum arising residual stresses mainly conservative.

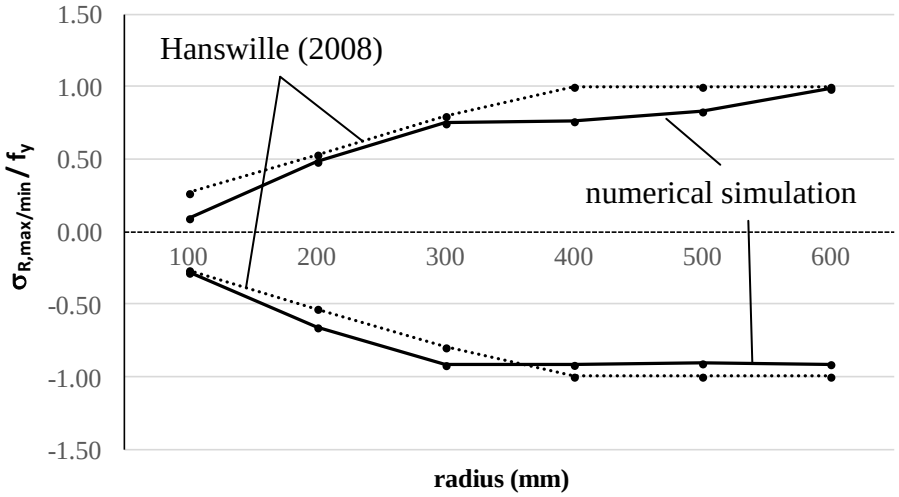

Fig. 6. Maximum and minimum residual stresses in massive circular steel sections.

Fig. 7 shows the stress distribution across the radius for various diameters. It is remarkable, that for all diameters the zone of zero residual stresses is located ≈ 0.25-0.3·r from the outer edge. This correlates to the parabolic approximation by Hanswille. On the other hand, the shape of the distribution in between only suites good to the parabolic approximation for large diameters. For small diameters especially the tensile zone in the centre flattens and does not match to the proposed distribution.

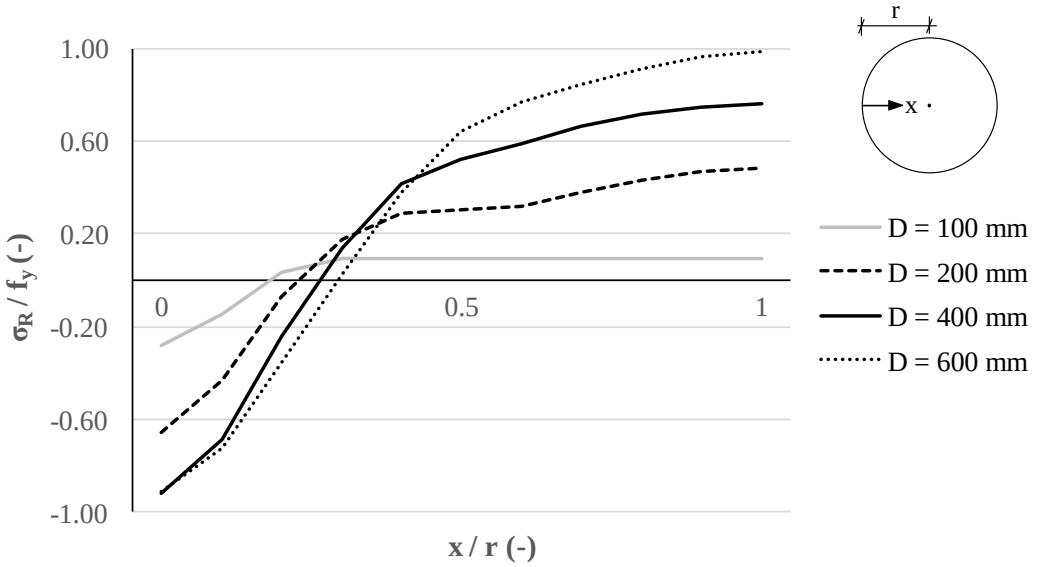

Fig. 7. Residual stress distribution along the radius of massive circular steel profiles.

Both compared criterions, the maximum and minimum amount and the distribution of residual stresses, showed that the quadratic approximation is suitable as a simplified estimation. Nevertheless, a main criticism of this approach is, that it does not fulfill the basic characteristic of residual stresses whereas all stresses are in balance. Performing a preliminary coupled thermal-mechanical simulation and transferring the resulting stress

distribution to the main model, this characteristic is fulfilled. In doing so, it is capable to consider both structural and geometrical imperfections.

3. SUMMARY

In this work, a detailed description of a 3D numerical model of a composite column with embedded massive steel core in case of fire is presented. A coupled thermal-mechanical analysis is performed, which considers both material and geometrical non-linearities. The mechanical contact is defined as hard contact in normal direction and via Coulomb friction in tangential direction. Furthermore, sensitivity studies carried out to identify suitable thermal contact properties are performed and shortly presented.

The load introduction is carried out using a uniformly loaded loading plate connected to the column to avoid numerical instabilities. Both geometrical and structural imperfections are introduced to the model. The approximation of residual stresses via simplified approaches is compared to the results coming from a preliminary analysis.

REFERENCES

ABAQUS. 2010. *Abaqus/Standard Version 6.10*. Pawtucket: Hibbit, Karlsson & Sorensen, Inc.

DIN EN 1994-1-2/NA 2010. Nationaler Anhang - National festgelegte Parameter - Eurocode 4: Bemessung und Konstruktion von Verbundtragwerken aus Stahl und Beton – Teil 1-2: Allgemeine Regeln – Tragwerksbemessung für den Brandfall. Deutsches Institut für Normung, Beuth Verlag, Berlin.

Ding J, Wang YC. 2008. Realistic modelling of thermal and structural behaviour of unprotected concrete filled tubular columns in fire. *Journal of Constructional Steel Research* 64:1086-1102.

Ehm C. 1986. Versuche zur Festigkeit und Verformung von Beton unter zweiachsialer Beanspruchung und hohen Temperaturen. Forschungsbericht, Heft 71. Braunschweig: Institut für Baustoffe, Massivbau und Brandschutz, Technische Universität Braunschweig.

EN 1994-1-2 2010. Eurocode 4: Design of composite steel and concrete structures – Part 1-2: General rules - Structural fire design. European Committee for Standardisation, Brussels.

Goralski C. 2006. *Zusammenwirken von Beton und Stahlprofil bei kammerbetonierten Verbundträgern*. PhD thesis. Rheinisch-Westfälische Technische Hochschule Aachen.

Grassl P, Jirasek M. 2006. Damage-plastic model for concrete failure. *International Journal of Solids and Structures* 43:7166-7196.

Hamme U, Schaumann P. 1987. Rechnerische Analyse von Walzeigenspannungen. *Stahlbau* 56:328-334.

Hanswille G, Lippes M. 2008. Einsatz von hochfesten Stählen und Betonen bei Hohlprofil-Verbundstützen. *Stahlbau* 77:296-307.

Hong S, Varma A. H. 2009. Analytical Modeling of the Standard Fire Behavior of Loaded CFT Columns. *Journal of Constructional Steel Research* 65:54–69.

Johansson M, Gylltoft, K. 2002. Mechanical Behaviour of Circular Steel-Concrete Composite Stub Columns. *Journal of Structural Engineering*. 1073-1081.

Lubliner J, Oliver J, Oller S, Onate E. 1989. A plastic-damage model for concrete. *International Journal of Solids and Structures* 25:299-326.

Schaumann P, Kodur V, Bahr O. 2009. Fire Behaviour of hollow structural section steel columns filled with high strength concrete. *Journal of Constructional Steel Research* 65:1794-1802.

Wohlfahrt H. 2001. Simulation der Vorgänge im Schmelzbad beim Laserstrahlschweißen zur Voraussage von Nahtausbildung, Gefüge, Verzug und Schweißeigenspannungen. Forschungsbericht. Braunschweig: Institut für Schweißtechnik, Technische Universität Braunschweig.

TECHNICAL SHEET 3

ADVANCED NUMERICAL MODEL FOR THE FIRE BEHAVIOUR OF COMPOSITE COLUMNS WITH HOLLOW STEEL SECTION

C. Renaud and G. Bihina

(Centre Technique Industriel de la Construction Métallique, France)

ADVANCED NUMERICAL MODEL FOR THE FIRE BEHAVIOUR OF COMPOSITE COLUMNS WITH HOLLOW STEEL SECTION

An advanced 2D finite element model developed at CTICM is presented to simulate the mechanical behaviour and resistance of both steel-concrete composite members and frames exposed to fire. This model is built from specific multi-fibre beam finite elements. In particular, it allows taking into account the interaction between the hollow steel section and the concrete core resulting in slip at the steel-concrete interface of composite columns exposed to fire. Both geometrical and material non-linearities as well as temperature distribution through the cross-sections and over the length of columns can be also considered. Comparisons of numerical calculations made using the model with 33 fire resistance tests carried out in France, in Germany and in Canada show that the model is able to predict the fire resistance, expressed in minutes of fire exposure, of composite columns with a good accuracy.

1. INTRODUCTION

During the last 30 years extensive experimental and theoretical investigations on the fire performance of unprotected steel hollow sections filled with concrete have been carried out in the world (Grimault 1980, Kordina & Klingsch 1983, Klingsch & Wittbecker 1988, Lie & Caron 1988a,b, Lie & Chabot 1992, 1994). Calculation methods have been developed to predict the fire resistance of structures and structural elements. When well calibrated to experimental results such methods prove to be a practical alternative to testing structures subject to fires which is costly. In these methods the thermal and structural behaviour of composite structures under fire conditions are assumed to be uncoupled. For the purpose of the structural analysis, temperature distributions in columns are obtained separately, either from heat transfer analysis or from test data. The structural behaviour of the member is then determined in a step by step procedure using the temperature distribution provided at each time step taking into account the influence of temperature on the mechanical properties of materials.

The present technical sheet is devoted to present a finite element model specifically for simulating the mechanical behaviour and resistance of both steel-concrete composite members and frames exposed to fire. In particular, this model is able to simulate the interaction between the hollow steel section and the concrete core resulting in slip at the steel-concrete interface. This is achieved by choosing the slip as an additional nodal degree of freedom. In addition to different structural configurations of columns (isolated or as a part of a frame) both geometrical and material non linearities as well as temperature distribution through the cross-sections and over the length of the columns can be taken into account.

After a short presentation of the main characteristics of the model, a comparison is performed between French, German and Canadian fire test results and corresponding calculation results.

2. PRESENTATION OF EFFICIENT NUMERICAL MODEL

The model presented in this work is an advanced calculation model developed at CTICM (Renaud et al. 2000, 2002, 2003, Renaud 2003). In fact, this model based on the finite element method is applicable not only to steel-concrete composite columns but also to complex planar composite frames subjected to any fire conditions.

2.1. BASIC FORMULATION

The formulation used in the model and the assembly of finite elements are based on the principle of virtual work expressed in an Updated Lagrangian Description; they refer to the configuration of the structure at time t to solve the equilibrium problem at time (t+Δt), the resolution being necessarily of incremental type.

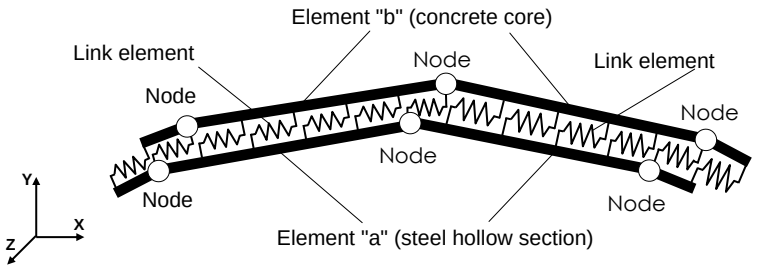

Fig. 1. Specific composite bar element.

Any composite column whose flexural bending occurs in a symmetrical plane may be idealised as an assemblage of three specific finite elements (Fig. 1), namely:

- a first beam-column element for some length of the steel hollow section (superscript (a)) with a node at each end and three degrees of freedom at each node;
- a second beam-column element for the concrete core (superscript (b)) corresponding to the same initial length as the steel element and having also two nodes; and
- a two-node link element with zero thickness and only one degree of freedom at each node corresponding to the discretisation of the distributed shear connection between the steel and concrete beam-column elements.

The cross-section of the resulting bar element is subdivided into small fibres which can be triangular, quadrangular or both. The material behaviour of each fibre is calculated at the centre of the fibre and is considered to be constant for the whole fibre.

Bernoulli's assumption is adopted for the cross-section of the above-mentioned bar elements and any gap between the hollow steel section and the concrete core is neglected so that the unknown variables at node i used to solve the global equilibrium problem can be reduced to:

$$\{\Delta D_i\} = \left[\Delta u_i^{(a)}, \Delta v_i^{(a)}, \Delta \theta_i^{(a)}, \Delta \gamma_i\right]^T \quad (1)$$

where:

- $\Delta u_i^{(a)}, \Delta v_i^{(a)}, \Delta\theta_i^{(a)}$ are the increments, between t and (t+Δt) , of the usual nodal variables referred to the global coordinate system of the column and related to the translational displacement in X direction, the translational displacement in Y direction and the rotation around Z axis, respectively;
- $\Delta\gamma_i$ is a nodal variable which corresponds to the increment of relative displacement between the steel and concrete parts, at node i in the tangential direction to the interface considering the configuration at time t.

Consequently, the variables are referred to a generalised global coordinate system needing a further treatment to establish the iteration equilibrium matrix equation of the whole composite element.

In addition to the large change of configuration of the column (isolated or included into a frame), several non-linearities should be taken into account due to the behaviour of materials (structural steel, concrete and shear connectors) depending on the temperature variation. In the presence of a temperature distribution in any cross-section, it is generally assumed that the total strain of every fibre of both elements (steel and concrete) is given by the sum of four independent terms, namely:

$$ {}_t\varepsilon_T = {}_t\varepsilon_\sigma + {}_t\varepsilon_{th} + {}_t\varepsilon_r + {}_t\varepsilon_{cr} \tag{2}$$

where ${}_t\varepsilon_T$ is the total strain at time t; ${}_t\varepsilon_\sigma$ is the instantaneous strain related to the stress exerted on the fibre at the relevant temperature; ${}_t\varepsilon_{th}$, ${}_t\varepsilon_r$ and ${}_t\varepsilon_{cr}$ are the strains due to thermal elongation, residual stress and creep, respectively. Obviously, the distribution of ${}_t\varepsilon_T$ in each part (steel or concrete) of the cross-section must respect Bernoulli's principle.

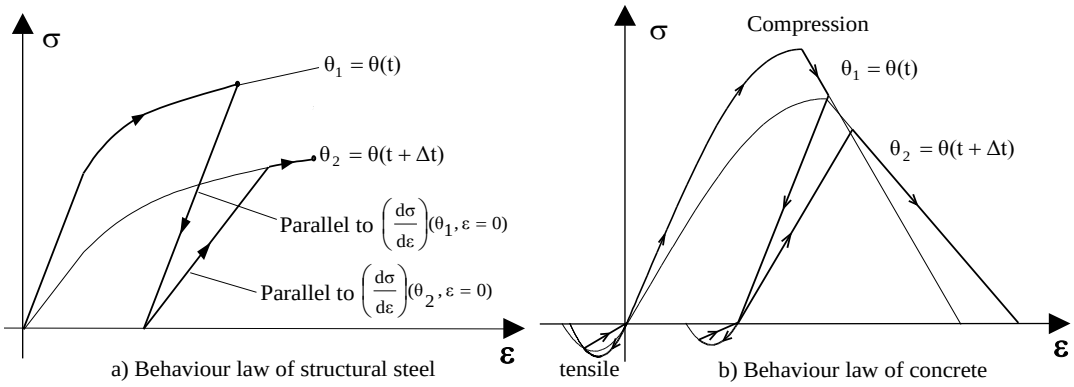

Fig. 2. Procedure to change from a stess-strain curve to another.

In principle, the model can take into account any stress-strain relationship. However, material properties recommended in Eurocode 4 Part 1-2 (CEN (2006)) are generally adopted here to remain consistent with this code.

Material properties are temperature dependant. Thus, from one temperature to another, the strain-stress curve is different for the same material. Consequently, a specific procedure is used to change from a behaviour curve to another, at each step of time and thus of temperature (see Fig. 2**)**. It consists in keeping the value of the permanent strain data from a virtual unloading at time t (also this unloading may be simplified for concrete in tension).

As additional simplification, generally a uniform temperature is assumed over the entire column length, reducing the thermal analysis to a two-dimensional problem of transient heating through the cross-section only, which can be solved numerically using either a finite difference method or a finite element approach.

2.2. GLOBAL EQUILIBRIUM EQUATION

The application of the finite element method within an Updated Lagrangian Description to any structure, after assembling the various composite bar elements and taking into account the boundary conditions, leads to the global equilibrium matrix equation of the structure which can be expressed only in the following incremental form:

$$\left[{}^{t}_{t}\mathrm{K}\right]\left\{\Delta \mathrm{D}^{(k)}\right\}=\left\{{}^{t+\Delta t}\mathrm{S}\right\}-\left\{{}^{t+\Delta t}_{t+\Delta t}\mathrm{F}_{\mathrm{G}}^{(k-1)}\right\}+\left\{\Delta_{t}\mathrm{F}_{\mathrm{th,cr,r}}^{(k)}\right\}, \quad (3)$$

and is associated with a Newton-Raphson iteration process for resolution.

In equation (3):

- $\left[{}^{t}_{t}\mathrm{K}\right]$ is the tangential stiffness global matrix of the structure;
- $\left\{\Delta \mathrm{D}^{(k)}\right\}$ is the incremental vector of generalised nodal displacements at iteration (k);
- $\left\{{}^{t+\Delta t}\mathrm{S}\right\}$ is the vector of nodal external forces at time $(t+\Delta t)$;
- $\left\{{}^{t+\Delta t}_{t+\Delta t}\mathrm{F}_{\mathrm{G}}^{(k-1)}\right\}$ is a vector of equivalent nodal forces resulting from the work of internal forces due to the change of configuration (including the internal forces of the discretised shear connection), corresponding to time $(t+\Delta t)$ and iteration (k-1);
- $\left\{\Delta_{t}\mathrm{F}_{\mathrm{th,cr,r}}^{(k)}\right\}$ is also a vector of equivalent nodal forces due to the strain increases, between t and $(t+\Delta t)$, resulting from thermal expansion (subscript th), creep (subscript cr) and possible residual stresses (subscript r) in the materials.

In fact, the right member of equation (3) represents an "out-of-balance" between the external and internal nodal forces. Once equation (3) is solved, the displacements should be adapted as follows:

$$\left\{{}^{t+\Delta t}\mathrm{D}^{(k)}\right\}=\left\{{}^{t+\Delta t}\mathrm{D}^{(k-1)}\right\}+\left\{\Delta \mathrm{D}^{(k)}\right\} \quad (4)$$

Adopting $\left\{{}^{t+\Delta t}\mathrm{D}^{(0)}\right\}=\left\{{}^{t}\mathrm{D}\right\}$ in relationship (4), the iteration process is performed for k=1,2,3..., until the "out-of-balance" in equation (3) is negligible within a certain convergence measure.

3. COMPARISON OF THE MODEL WITH FIRE TESTS

Thirty-three fire tests are considered here (see Table 1) which were carried out in France (Fire station of CTICM in "Maizières-Les-Metz"), in Germany (University of Braunschweig) supported by CIDECT research projects (Kordina & Klingsch 1983) and in Canada (Institute for Research in Construction, National Research Council of Canada).

Table 1. Structural properties and failure times of tested columns.

Test	Profile Type	Rebars	Length (mm)	End Conditions	Test Loading		Material properties (N/mm²)			Measured failure time (min)	Maximum temperature in steel (°C)
					Load (KN)	Eccentricity (mm)	Steel	Rebars	concrete		
1	200×6.3	4ϕ18	4200	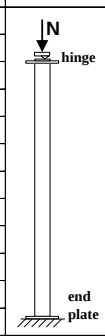	432	20	277	475	45.9	63	975
2	200×6.3	4ϕ18	4200		318	50	277	475	45.9	58	950
3	200×6.3	4ϕ18	4200		537	5	291	475	42.9	61	950
4	200×6.3	4ϕ18	3700		649	20	300	475	55	39	880
5	200×6.3	-	4200		400	20	279	-	55	22	750
6	200×6.3	4ϕ18	3700		649	20	265	475-	75	56	1010
7	200×6.3	4ϕ18	4200		550	5	274	475	75	59	1035
8	200×6.3	4ϕ18	3700		294	20	281	469	35	82	1100
9	200×6.3	4ϕ18	4200		375	22	287	469	35	68	920
10	200×12.5	4ϕ18	4200		453	50	234	475	45.9	34	775
11	300×7.0	8ϕ14	3621		1500	50	327	441	38	57.3	780
12	300×7.0	8ϕ14	3619		1500	100	327	441	38	25	600
13	150×5.0	4ϕ12	3810	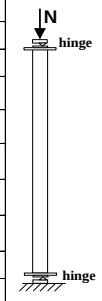	140	0	416	596	37.8	82	1010
14	200×5.0	8ϕ10	3600		500	7	378	494	38.5	62	830
15	200×5.0	4ϕ10	3600		500	15	378	494	38.5	56.4	830
16	200×5.0	4ϕ6	3490		1000	0	598	500	32.5	23	600
17	200×10.0	4ϕ6	3430		1200	5	598	500	36.5	27.1	600
18	273.1×6.35	4ϕ20	3810		1050	0	350	400	46.7	188	1050
19	273.1×6.35	4ϕ20	3810		1900	0	350	400	47.0	96	930
20	300×7.0	8ϕ20	3600		1870	0	331	441	32.5	136	1030
21	300×7.0	8ϕ20	3600		2570	0	331	441	32.5	59	840
22	300×8.0	4ϕ32	3810		1400	66	394	596	43.8	58	920
23	168.3×4.8	-	3810	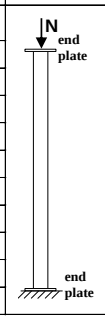	150	0	350	-	32.7	76	910
24	168.3×4.8	-	3810		150	0	350	-	35.4	81	930
25	203×6.35	4ϕ16	3810		930	0	350	400	48.1	105	945
26	219.1×4.78	-	3810		492	0	350	-	31.0	80	925
27	219.1×4.78	-	3810		384	0	350	-	32.3	102	960
28	254×6.35	4ϕ20	3810		1440	0	350	400	48.1	113	990
29	254×6.35	4ϕ20	3810		2200	0	350	400	48.1	70	880
30	273.1×5.56	-	3810		574	0	350	-	28.6	112	955
31	273.1×5.56	-	3810		525	0	350	-	29.0	133	985
32	273.1×5.56	-	3810		574	0	350	-	27.2	70	860
33	355.6×12.7	-	3810		1050	0	350	-	25.4	170	1030

3.1. ASSUMPTIONS FOR NUMERICAL SIMULATIONS

The following assumptions were made:

- The thermal and mechanical materials properties as a function of temperature were taken to be in accordance with EC4 Part 1-2. It may be underlined that the creep strains of steel and concrete are implicitly included in the stress-strain relationships at elevated temperature;
- Temperature distributions were introduced either from a 2D heat transfer analysis or test data. Over the height of the column a uniform temperature has been assumed for the German tests. With regard to the French and Canadian tests, a temperature gradient at the top of the columns has been taken into account over about 300 mm. This temperature gradient was due to the fact that the top of the column, being outside the furnace during the test, was not heated directly by fire but by conduction;
- All the columns were tested without measuring their out-of-straightness. An out-of-straightness of L/500 was however used in the numerical simulations (tolerance

given by the manufacturer). It was considered to be always on the side leading to a cumulative effect with the loading eccentricity;
- The mechanical interaction between the hollow steel section and the concrete core has been neglected: slipping has been assumed to occur without significant bond between the steel tube and the concrete core.

To illustrate the effects of end restraint conditions of columns and of slip at the steel-concrete interface, the behaviour of Test 1 (see Table 1) is simulated with or without slip and with two different end conditions (namely hinged at both ends or fixed at one end and hinged at the other end). For this test, the temperature measurements in several points of the section have allowed to introduce directly a temperature field of sufficient accuracy into the numerical simulation.

At ordinary temperature, the column was designed as hinged at both ends. Assuming the same support conditions during the fire, the calculated failure time of the column is equal to 19 minutes, which is very far from the test failure time (63 minutes). In reality, observation of the bending deflection of the column after the test has suggested to try other support conditions, namely a hinged support at the bottom and a restraint condition at the top. Using these new support conditions, the failure time becomes 61 minutes, which now is close to the time measured. Generally, for single columns ended with head and foot plates or bearings, it is assumed that the support conditions are hinged. As explanation of the above result appearing opposite, it is presumed that additional restraints may result from the parts of the structure only partially affected by the fire temperature above and below the column ends and therefore having a higher stiffness.

The evolutions of the vertical displacement calculated at the top of the column and of the transverse deflection calculated at mid-height of the column are shown in Fig. 3 and Fig. 4, respectively. These displacements are compared to the measured ones. In the case of restraint condition at the top, there is a good agreement between measured and calculated displacements, in particular when the slip is taken into account.

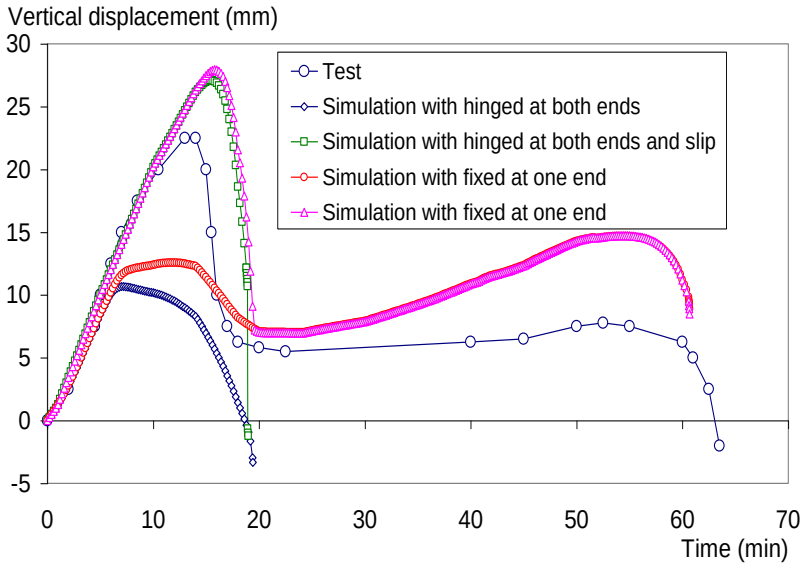

Fig. 3. Vertical displacement at the column top.

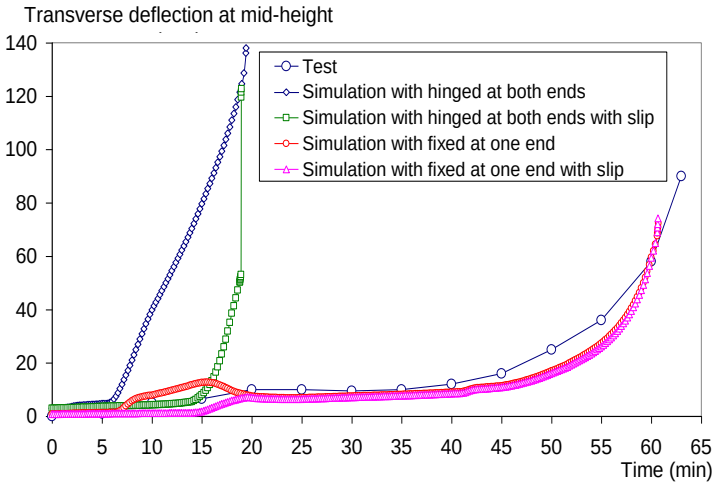

Fig. 4. Transverse deflection at mid-height of column.

Whereas the transverse deflection calculated at mid-height is practically the same as the one measured, it should be noted that column elongation is somewhat over-estimated near the end of the test. Likely an explanation of this difference may be found in the fact that the column is not uniformly overheated on its whole length. In addition, introducing into the calculations the temperatures directly measured in some points of cross-sections may involve an over-estimation of unknown temperatures inside the concrete, and consequently a more important expansion of the latter. It should be noted that a difference exists again in the neighbourhood of the fifteenth minute, which may be explained by certain bond persistence between the steel tube and the concrete core, in spite of the important rise of temperature. Excepting the first 30 minutes, the slip does not seem to have a significant influence on the column deformation, and consequently on the time of fire stability.

3.2. SYNTHESIS OF RESULTS

Calculations have been performed dealing with the 33 column tests carried out in France, Germany and Canada. Globally the difference between failure times ascertained numerically and experimentally does not exceed 15% as illustrated in Fig. 5, which is fully acceptable considering the various uncertainties inherent to test data, such as the heating condition along the height column, the degree of rotational restraint at the column ends, the unintentional eccentricity of axial load, the initial out-of-straightness of the column, etc. The good agreement of the model in comparison with tests is due not only to the choice of appropriate material laws as well as introduction of column imperfections (initial out-of-straightness, residual stresses) but also to the ability to take into account the phenomenon of slip between the steel tube and the concrete core.

All the numerical results confirm that the slip has no significant influence on the failure time of composite columns, provided that the hollow section is filled with reinforced concrete. However it leads to a more realistic evolution path of the displacements (vertical displacement and deflection) during the first period of heating as already shown in Fig. 3. On the contrary, columns without reinforcement and columns subjected to important bending moments appear to be more sensitive to the phenomenon of slip which may influence not only their deformations but also their failure time.

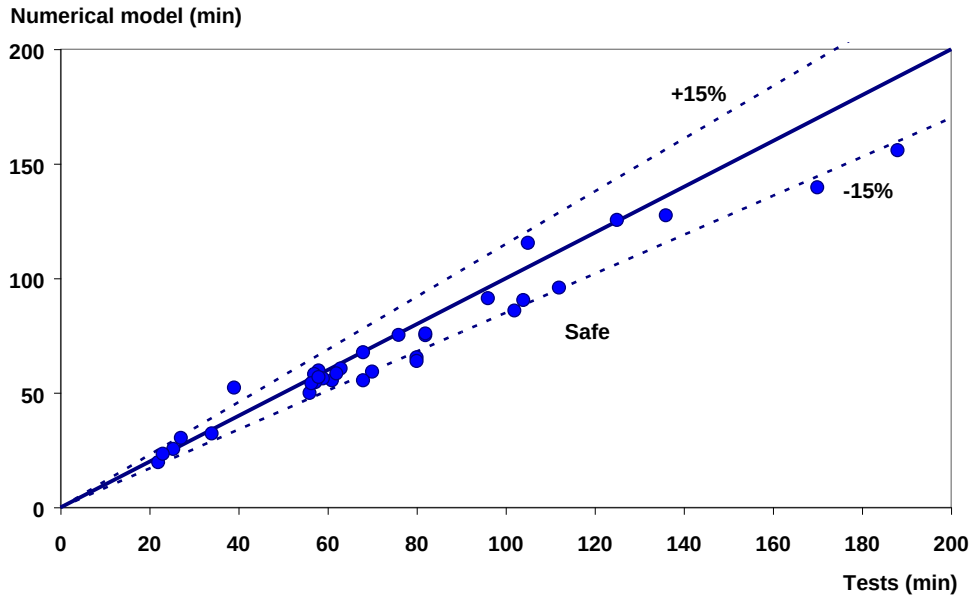

Fig. 5. Comparison of fire resistances between the numerical model and tests.

4. CONCLUSION

The main features of a finite element model specifically to analyse the fire resistance of composite structures taking into account the effect of the interface slip between steel and concrete have been presented. Using this model, the fire resistances of several composite columns with concrete filled hollow steel sections have been calculated and compared with test results. These comparisons show that the model can simulate appropriately the structural behaviour of composite columns and provide a good estimation of the fire resistance time.

The model was then used to perform a very wide series of numerical simulations for many values of significant parameters affecting the performance of composite columns such as buckling length, fire duration, cross-section size, etc., and considering the standard fire exposure. On the basis of numerical results, a more suitable simplified method was established as an alternative to that given in Annex G of Eurocode 4 (CEN 2006). Indeed, in the latter method which has proven to be unsafe for intermediate slendernesses (Twilt & Haar (1984, 1985)), the effects of restrained thermal stresses and initial deflection of the columns on their load bearing capacity are entirely neglected. These effects can become important for columns with high buckling lengths; therefore, they are taken into account globally in the simple method deduced from the numerical model presented in this work. Once validated, this method has been included in the French National Annex of the current version of Eurocode 4 Part 1-2.

REFERENCES

Grimault JP. 1980. *Détermination de la durée au feu des profils creux remplis de béton*, Rapport final établi par COMETUBE. Commission des Communautés Européennes, Recherche Technique Acier, Paris.

Klingsch W, Wittbecker FW. 1988. *Fire resistance of hollow section composite columns of small cross sections*. Bergische Universität, Wuppertal, West Germany.

Kordina K, Klignsch W. 1983. *Fire resistance of composite columns with concrete filled hollow sections*, Research report, CIDECT 15 C1/C2 – 83/27.

Lie TT, Caron SE. 1988a. *Fire resistance of circular hollow steel columns filled with siliceous aggregate Concrete*. Test results, internal report n°570. Institute for research in Construction, NRCC, Canada.

Lie TT, Caron SE. 1988b. *Fire resistance of circular hollow steel columns filled with carbonate aggregate Concrete*. Test results, internal report n°573. Institute for research in Construction, NRCC, Canada.

Lie TT, Chabot M. 1992. *Experimental studies on the fire resistance of hollow steel columns filled with plain concrete.* Internal report 611. Institute for research in Construction, NRCC, Canada.

Lie TT, Chabot M. 1994. *Fire resistance tests of square hollow steel columns filled with reinforced concrete*, Test results, Internal report n°673. Institute for research in Construction, NRCC, Canada.

Renaud C, Aribert JM, Zhao B. 2000. Fire stability of steel-concrete composite columns with hollow steel section made in high strength steel. *French Journal of Steel Construction* 3:5-18.

Renaud C, Aribert JM, Zhao B. 2002. Proposal of a simple calculation model for the fire resistance of concrete filled hollow section columns. *Proceedings of third European conference on steel structures*, Vol. 2, 1355-1366.

Renaud C, Aribert JM, Zhao B. 2003. Advanced numerical model for the fire resistance of composite columns with hollow steel section. *Steel and composite structures:* 2(3):75-95.

Renaud C. 2003. *Modélisation numérique, expérimentation et dimensionnement pratique des poteaux mixtes avec profil creux exposés à l'incendie*. Thèse de Docteur en génie civil. INSA de Rennes, France.

Renaud C, Zhao B, Kruppa J. 2003. *Improvement and extension of the simple calculation method for fire resistance of unprotected concrete filled hollow columns*. CIDECT research project 15Q. CTICM ref. insi-04/075b-CR/PB 2003.

CEN. 2006. *Eurocode 4 Part-1-2, Design of composite steel and concrete structures: Structural fire design*.

Twilt L, Haar PW. 1984. *Analysis of the discrepancy between the French and German calculation methods for the fire resistance of concrete filled steel columns*. IBBC-TNO-report n° B-84-480, September.

Twilt L, Haar PW. 1985a. *The effect of the mechanical properties and the thermal induced stresses on the discrepancy between the French and German calculation methods for the fire resistance of concrete Filled steel columns*. IBBC-TNO-report n° B-85-93, March.

Twilt L, Haar PW. 1985b. *The discrepancy between the French and German calculation methods for the fire resistance of concrete filled steel columns: Proposition for harmonisation*. IBBC-TNO-report n° B-85-426, August.

TECHNICAL SHEET 4

NUMERICAL ANALYSIS OF COMPOSITE STEEL-CONCRETE COLUMNS UNDER FIRE CONDITIONS

L.M.S. Laím, J.P. Rodrigues, A.M. Correia and T.A. Pires

(Universidade de Coimbra, Portugal)

NUMERICAL ANALYSIS OF COMPOSITE STEEL-CONCRETE COLUMNS UNDER FIRE CONDITIONS

The finite element method acts as a link between experimental studies and analytical models, enabling a better understanding of the behaviour and experimental control to obtain simplified methods. The modelling of composite steel-concrete columns, presents a high level of complexity to treat some specific phenomena such as cracking of concrete, spalling, local buckling of the steel profile, complex interaction between steel and concrete, and welding behaviour between the steel profile and stirrups. The main objective of this work is to present a three-dimensional nonlinear finite element model in order to predict the behaviour of composite columns in fire, considering the restraint of columns to their thermal elongation. The validation of the proposed model is investigated comparing numerical with experimental results obtained from fire resistance tests conducted on composite columns with restrained thermal elongation at the University of Coimbra, in Portugal.

1. INTRODUCTION

The behaviour of composite columns made of partially encased steel sections subjected to fire has been numerically investigated by several authors, especially in the last decade, but even so only a few experimental studies have been published on these types of columns with restrained thermal elongation. In 2006, Wang et al. (Wang & Tan 2006) presented a design concept called the residual area method to calculate the equivalent thickness of concrete for temperature analysis of concrete-encased I-sections in fire. The steel temperature response of concrete-encased I-sections subjected to fire is characterized by three temperature variables. The proposed method makes use of the EN1993-1.2 (2004) provisions to formulate the temperature response of each representative point along the steel profile using a 1D heat transfer model. The results demonstrate that the residual area method is intrinsic to the geometric configurations (cross sections) of concrete-encased I-sections, but independent of heating conditions. The proposed method has been further verified by three series of specimens, and the predictions are compared against the results obtained from finite element analysis. In 2007 and 2008, Huang et al. (Huang et al. 2007a, 2007b, 2008) presented a numerical study on the fire resistance of embedded I-section composite columns. The objective was to examine the effects of the cross-sectional dimensions and load level on the column fire resistance. Four groups of columns, consisting of square cross-section were used. The columns were subjected to axial compression forces and four-side uniform heating. Four load levels were studied: 0.2, 0.3, 0.4 and 0.5. These load levels were a percentage of the design load capacity at ambient temperature, calculated according to EN1994-1.1 (2003). They concluded that, under high loading levels, columns with small cross-sections fail to meet the fire resistance as suggested by EN 1994-1-2 (2005). The authors state clearly in this work that their study was limited to pin-ended columns, where boundary conditions have been oversimplified. An actual column within a building normally experiences limited axial and rotational restraints at its ends. Some studies have shown that the boundary restraints play a key role in the structural behaviour as well as fire resistance. In 2010, Ellobody et al. (Ellobody & Young 2010) presented a nonlinear 3-D finite element model for investigating the behavior of concrete encased steel columns at elevated

temperatures. The composite columns were pin-ended, axially loaded, having different load ratios during fire. The nonlinear material properties of steel, concrete, longitudinal and transversal reinforcing bars, as well as the effect of concrete confinement at ambient and elevated temperatures were taken into account. They have concluded that the fire resistance of the columns generally increases with the decrease in the column slenderness ratio, as well as the increase in the structural steel ratio. It was also shown that the time-axial displacement relationship is considerably affected by the coarse aggregate. Calculating the fire resistance with EN 1994-1-2 (2005), it was observed that Eurocode is conservative for all studied cases, except for the columns with a load ratio of 0.5 as well as columns having a slenderness ratio of 0.69 and a load ratio of 0.4. Also in 2010, Espinos et al. (Espinos et al. 2010) presented an advanced model for predicting the fire response of CHS columns. In this work, a nonlinear finite element three-dimensional model was presented and validated in order to study the behaviour of axially loaded of the mentioned type of columns exposed to fire. A realistic sequentially coupled nonlinear thermal-stress analysis was conducted for a series of columns. The model was validated by comparing the simulation results with fire resistance tests. By means of this model, an extensive sensitivity analysis was performed over a wide range of aspects concerning the finite element modelling of the problem. Based on this analysis, several modelling recommendations were presented. The validated numerical model was employed to study and discuss the EN1994-1.2 (2005) simple calculation model. This model does not take into account the effects of self-equilibrated thermal stresses and those of geometrical second-order local behaviour, which are crucial for the stability of the column. As the method is sectional, the strain in all the fibres within the cross-section of the column is assumed to be equal. This approach clearly neglects the effects of the differential longitudinal expansion between the steel tube and concrete core, thus assuming that a full bond occurs. As it is expected, all these factors lead to important deviations from the actual fire response of these columns. The numerical model showed good agreement with the tests both quantitative and qualitative. This research proved that Eurocode 4 simple calculation model may lead to unsafe results when working with columns with relative slenderness values over 0.4 and in general for pinned-pinned columns under concentric axial load.

Therefore, with the main purpose of obtaining, by the authors in the near future, analytical formulae for simplified design or verification of the fire resistance of innovative and slender concrete filled hollow columns, it is intended to describe in detail in this technical sheet all parameters, considerations and assumptions took into account in a three-dimensional nonlinear finite element model to predict the behaviour of composite columns in fire, such as, of columns previously tested in the laboratory by the authors. In this particular case of study, the experimental results were obtained from composite steel-concrete columns with restrained thermal elongation, which were made of partially encased H steel sections and of circular concrete filled hollow steel sections (CHS). The numerical results were thereby compared with those given by the experimental tests in order to validate the developed finite element model and to compare all those parameters, considerations and assumptions took into account in this model with the ones chosen by other researchers. This may make it possible to understand which parameters or assumptions have more influence on the analysis of this kind of numerical models.

2. EXPERIMENTAL INVESTIGATION

Fig. 1 represents a detailed scheme of the test set-up used at Coimbra University for carrying out the fire resistance tests on building columns with restrained thermal elongation, in which all the components are labelled. The system comprises a restraining steel frame of variable stiffness (1) with the function of simulating the stiffness of the surrounding structure to the column subjected to fire. The connections between these structural elements were performed with M24 bolts, grade 8.8, except the connections between the columns and upper beams (2) where threaded rods M27, grade 8.8, were used. Different hole positions in the flanges of the beams of the restraining frame, allowed the assembly of the columns in different positions, leading to different spans of the beams that corresponded to different values of the stiffness of the surrounding structure. The tested values of the axial stiffness were 13, 45 and 128kN/mm. The hydraulic jack of 3MN capacity (3) was controlled by a load cell of 1MN (4). It was fixed in the reaction frame (5) provided with a safety system (6). Four linear variable displacement transducers (LVDT) on bottom and three on top of the test columns (9) were used. The LVDT's were orthogonally arranged allowing the measurement of all deformation planes of the ends of the test columns and consequently their rotations. The lateral displacements of the column were measured by wire displacement transducers placed in two orthogonal directions, at 0.81m, 1.81m and 2.49m height in relation to the column base (10). Furthermore, an extra displacement transducer was placed in the centre of the 3D restraining frame, near the point of application of the load, to confirm the axial displacements of the test columns (11).

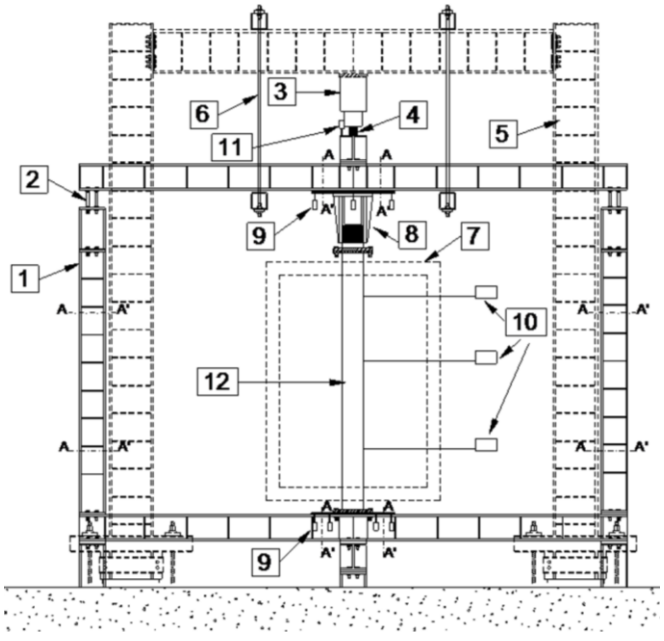

Fig. 1. Scheme of the test set-up.

The test column (12) was placed in the centre of the restraining frame and was properly fitted to it, in each end plate, with four steel bolts M24, class 8.8. A device to measure the restraining forces generated in the test columns (8) during the tests was built

with a hollow and stiff cylinder, rigidly connected to an upper beam, above the specimen. On top of the testing column, a massive steel cylinder was rigidly connected. The lateral surface of this cylinder was Teflon lined for preventing friction. This massive cylinder entered into the hollow cylinder, and pressed a load cell of 300kN inside the second, allowing with this to measure the restraining forces generated during the test. The thermal action was applied by a modular electric furnace (7) following approximately the standard ISO 834 fire curve (ISO 834, 1975). This furnace is composed of modules 1m height and one module 0.5m height, placed on top of each other forming a free chamber around the column of 1.5m x 1.5m x 2.5m. In each module, plate thermometers for controlling the furnace were positioned at mid-height.

3. NUMERICAL INVESTIGATION

The finite element program ABAQUS is a powerful computational tool for modelling structures with material and geometric nonlinear behaviour. Hence, ABAQUS (2010) version 6.10-1 was used extensively by the authors to develop a finite element model which aimed to simulate the behaviour and strength of composite steel-concrete columns under compressive loading conditions and fire in the experimental program carried out by Correia & Rodrigues (2011) and Pires et al. (2012).

3.1. GEOMETRY OF THE STUDIED SPECIMENS

Two different types of composite columns were selected for this study: rectangular and circular columns. The rectangular ones were made of a partially encased H-shaped steel profile (HEA) (Fig. 2). Two different HEA cross-sections were used for these profiles, where one was 152 mm tall and 160 mm wide (HEA160), and the other one was 190 mm tall and 200 mm wide (HEA200). Four steel bars with 16 mm in diameter were used as longitudinal reinforcement in the HEA160 cross-sections and four steel bars with 20 mm in diameter were used in the HEA200 cross-sections. On the other hand, the circular composite columns were made of a circular hollow steel profile (CHS) filled with reinforced concrete (Fig. 2). Two different external diameters were used for this type of columns, 168.3 and 219.1 mm, both ones with 6 mm of thickness. In addition, the columns with higher diameter had six longitudinal steel reinforcing bars with 12 mm in diameter, whereas the other ones had also six steel rebars, but with 10 mm in diameter. It is noticed that all these columns were 3000 mm tall and no stirrups were considered in this numerical model.

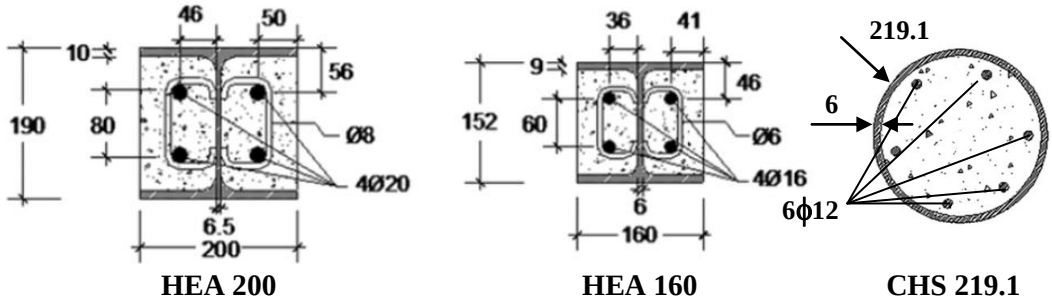

Fig. 2. Scheme of the cross-sections of the studied columns (dimensions in mm).

3.2. FINITE ELEMENT TYPE

All columns were modelled by using solid elements, C3D8RT, from the ABAQUS program library. This element is defined as a three-dimensional (3D), continuum (C), hexahedral and an eight-node brick element with reduced integration, i.e. one integration point for each surface of the element (R), hourglass control and first-order (linear) interpolation. These finite elements have three degrees of freedom per node, referring to translations in the three directions X, Y and Z (global coordinates). C3D8RT is also a temperature element (T). ABAQUS evaluates the material response at each integration point, namely, stresses and strains. The stresses at the nodes are interpolated or extrapolated from the integration points to the nodes. So, the reduced integration decreases the amount of CPU time necessary for analysis of the model. However, reduced integration elements converge non-monotonically and due to this reduced number of integration points hourglassing can occur, so an hourglass stabilization control feature is built into the element to suppress spurious modes.

3.3. FINITE ELEMENT MESH

The influence of the finite element size on the behaviour of the composite columns was first studied. It was found that good simulation results could be obtained by using an approximated 15 mm mesh size for the concrete parts and an approximately 25 mm mesh size for the steel profiles (Fig. 3). It is noticed that these finite element meshes were generated automatically by the ABAQUS program and used in all simulations. As the steel profiles are usually more rigid than the concrete parts, they are usually denoted as master surfaces in contact pairs and meshed coarser than the slave surfaces to increase the contact convergence rate.

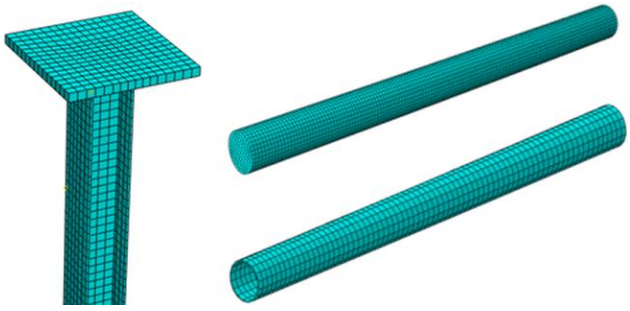

Fig. 3. Geometric parts divided into finite elements.

3.4. MATERIAL MODELLING

Material non-linearity in the specimens was modelled by using in these simulations the “plastic-plasticity” model for the steel and “concrete damaged plasticity” model for the concrete, from the ABAQUS program library. It is noticed that the reduction factors for the yield strength and the Young modulus of these materials at elevated temperatures, as well as their stress-strain relationships were obtained from the EN 1994-1-2 (2005). All steel profiles were made of S355 structural steel and the longitudinal steel reinforcement bars of S500 steel. Furthermore, all composite members presented a similar concrete composition with calcareous aggregate and C25/30 class. In relation to the

stress-strain relationship of the steel, true strain and stress were used directly as input data. Eurocode steel properties are given as engineering stress-strain input, which should be converted to true stress and true (logarithmic) strain using equations (1) and (2) where ε_{eng} and σ_{eng} are the engineering (nominal) strain and stress, respectively whereas ε_{true} and σ_{true} are the true strain and stress, respectively. All other components were modelled as elastic, i.e. the elastic modulus was equal to 210 GPa for the steel and to 31 GPa for the concrete, and the Poisson's ratio to 0.3 for the steel and 0.2 for the concrete at ambient temperature. However, this last value was assumed to remain unchanged with increasing temperature as well as the parameters which define the plastic behaviour of the concrete, including the dilation angle, the eccentricity, the ratio of initial equibiaxial compressive yield stress to initial uniaxial compressive yield stress, the *K* and the viscosity parameter. The dilation angle was taken as 35º whereas the other ones as 0.1, 1.16, 0.667 and 0, respectively, in other words, the default values given in the ABAQUS program library. Residual stresses were ignored in these analyses. Finally, the thermal properties of the respective materials at elevated temperatures considered in the model (mass density, expansion, thermal conductivity and specific heat) were also those established in EN 1994-1-2.

$$\varepsilon_{true} = \ln (1 + \varepsilon_{eng}) \quad (1)$$

$$\sigma_{true} = \sigma_{eng} (1 + \varepsilon_{eng}) \quad (2)$$

3.5. FINITE ELEMENT MODEL

3.5.1. Geometric properties

A three-dimensional numerical model was used to describe all buckling modes observed in the experimental tests (Correia & Rodrigues 2011 and Pires et al. 2012). Such as observed in the real test set-up, a three-dimensional frame was performed to take into account not only the axial stiffness but also the rotational stiffness of the surrounding structure to the column (Fig. 4). Different values of stiffness were provided by positioning the peripheral columns of the restraining frame in different positions. With different values of the span, different values of axial and rotational stiffness were obtained.

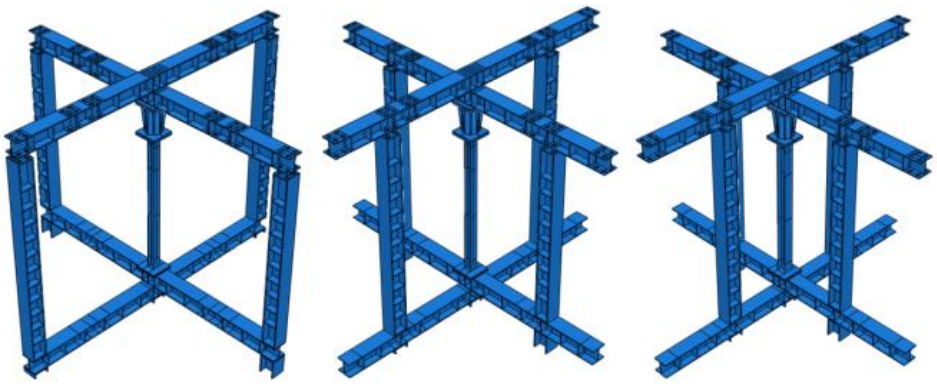

Fig. 4. Numerical model used in the finite element analysis.

3.5.2. Contact configuration

It was assumed a tangential friction coefficient of 0.2 for the contact behaviour in tangential direction and a hard contact (full transmission of compressive forces and no transmission of tensile forces) for the contact behaviour in normal direction, between the steel profile and the concrete (Fig. 5a). The surface to surface contact method was used, because this one gives a good convergence rate and it is much less sensitive to the choice of master and slave surfaces. As well as that, the penalty method was defined as the contact property between the steel and the concrete. All other connections of the restraining frame and between the longitudinal reinforcement and the concrete were modelled using *TIE Constraints option in ABAQUS (Fig. 5b). This method combines the two parts in all degrees of freedom at the connected region. Such simplification significantly reduces additional contact configuration and converging challenges.

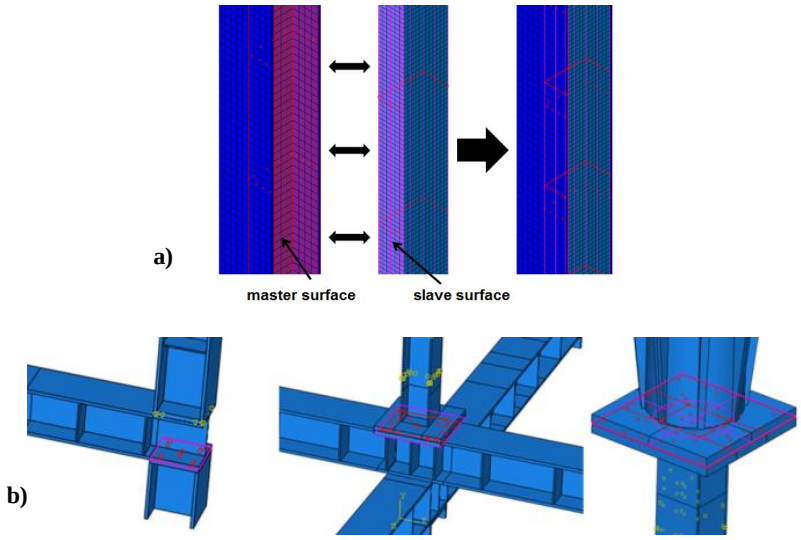

Fig. 5. Contact between steel profile and reinforcing concrete (a) and between parts of restraining frame (b).

3.5.3. Thermal action

The thermal action was applied on the testing column, at different heights, because it was observed in the tests a great temperature gradient along the vertical direction, in the gas inside the furnace. So, to reproduce as faithful as possible the test conditions, the column was partitioned into three parts (Fig. 6), two with 1m of height and one with 0.5m, in accordance with the modular furnace dimensions. The fire action was defined in ABAQUS program by two types of surface, namely, “film condition” and “radiation to ambient”, corresponding respectively to heat transfer by convection and radiation. Radiation was considered with a resultant emissivity of 0.56 for steel and 0.49 for concrete.

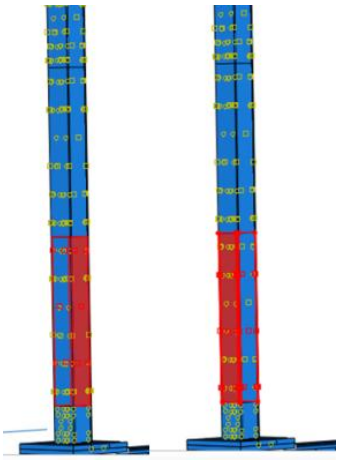

Fig. 6. Thermal action applied on the column.

In other words, the emissivity of the furnace's electric resistance and the emissivity of the steel and the concrete were taken as 0.7, 0.8 and 0.7, respectively. Finally, convection was considered with a coefficient of heat transfer by convection equal to 25 w/m^{2}ºC, as recommended by EN1991-1-2 (2002). Lastly, a conduction coefficient of 200 W/m^{2}K was adopted in the contact between the steel profile and the concrete.

3.5.4. Boundary and loading conditions

Regarding the boundary conditions, all degrees of freedom of the nodes located on the bottom surface of the supports of the restraining frame were constrained and the initial temperature of all nodes of the numerical model was taken as 20 ºC. The load was applied on top of the upper beam, in several points, to prevent excessive deformation of the upper flange. The load level applied on the beams was a percentage (30 and 70%) of the design value of buckling load of the columns at ambient temperature, calculated in accordance with the methods proposed in EN 1994-1-1 (2003). The loading intended to simulate the serviceability load of a column when this one is inserted in a real building structure. Geometric imperfections were also considered as a bow out-of-straightness of *L*/1000 (where *L* is the length of the column) at mid-height of the column.

3.6. ANALYSIS METHOD

To achieve the goals of this numerical investigation, these simulations were performed in two stages: loading and heating stage. Firstly, a general static analysis was undertaken with the purpose of applying the load on the column. So, during this step, there was no constraint between the upper beams and peripheral columns of the restraining frame, in such a way that the beams could descend in vertical movement of translation, as a slide. Lastly, a coupled temperature-displacement analysis was undertaken in order to simulate the performance of composite columns under fire conditions until their failure. The nonlinear geometric parameter (*NLGEOM=ON) was set to deal with the geometric nonlinear analysis, namely, with the large displacement analysis.

3.7. VALIDATION OF FINITE ELEMENT MODEL

As results of these analyses, Fig. 7 represents the evolution of the temperature at mid-height of a circular and a rectangular composite column. It can be seen that differences between 10 and 20% were observed between the experimental and numerical results. However, these thermal results contribute for good results concerning the fire behaviour of the respective columns, as it can be seen in Fig. 8.

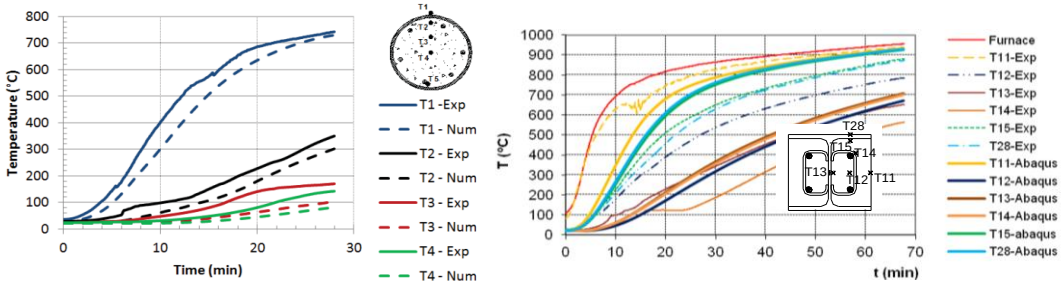

Fig. 7. Temperatures at middle height cross-section of the different columns.

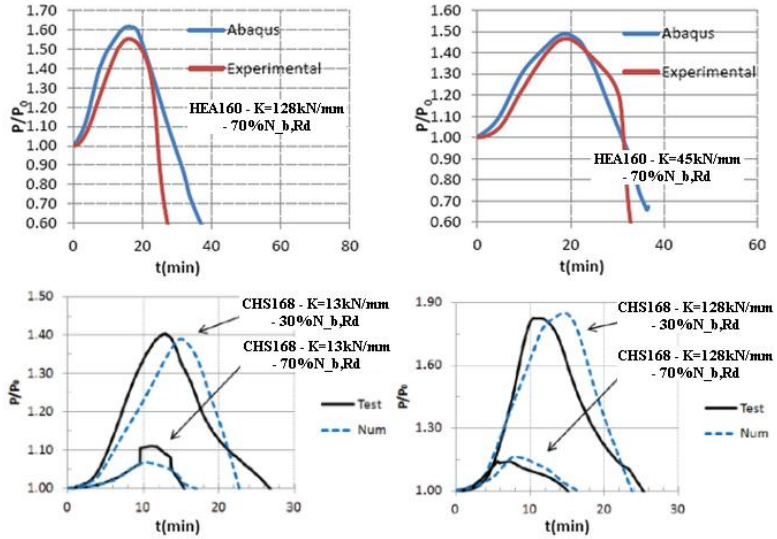

Fig. 8. Comparison of the evolution of restraining forces as a function of time obtained in numerical simulations and experimental tests.

In Fig. 8, it is shown the comparison of the evolution of restraining forces as a function of time obtained in numerical simulations and experimental tests. These graphs represent the typical behaviour of a real column inserted in a building structure, in which it is submitted to restraint to thermal elongation. Due to the effect of the thermal action, the axial force on the column begins to increase until it reaches a maximum value. After this maximum it begins to decline due to deterioration of mechanical properties of concrete and steel with temperature, reaching values lower than the initially applied load. It can be observed that the curves from finite element analysis (FEA) fit closely with the experimental curves, especially with the ones that presented high levels of initial applied load on the column.

3.8. FAILURE MODES OF THE COMPOSITE COLUMNS

Fig. 9 shows a representative view of the composite columns with partially encased H sections after fire tests. All tested specimens were observed to fail by global buckling. The absence of local buckling can be explained by the presence of concrete between flanges. This concrete is beneficial, not only in providing thermal insulation, but also in preventing local buckling of the flanges. The failure mode in most of the tested circular concrete filled hollow columns (CHS) was also global buckling (Fig. 10).

Fig. 9. Experimental (a) and numerical (b) configurations of a deformed composite H column after test.

Fig. 10. Experimental (a) and numerical (b) configurations of a deformed CHS column after test.

EN1994-1-1 (2003) states that the effects of local buckling may be neglected for a D/t ratio smaller than 59. All the columns presented here had a small ratio diameter-thickness D/t (i.e. 28 in 168.3mm and 37 in 219.1mm columns). Nevertheless several cases of local buckling were also observed. Comparing all results obtained, local buckling occurred more often in the following cases: (i) stiffness of surrounding structure of 13 kN/mm, (ii) load level of 70%, (iii) cross-section diameter of 219.1mm, (iv) CHS columns partially filled with concrete (concrete ring of different thickness around the internal surface wall of the steel tube), compared to those completely filled. The concrete filling avoiding local buckling, however concrete ring was not enough effective to prevent local buckling.

4. CONCLUSIONS

Some conclusions of this research were that (i) ABAQUS program simulated well the phenomenon of heat transfer between air and structural elements resulting from thermal actions; (ii) a good agreement may be observed between the results of the experimental tests and the numerical simulations, especially in what concerns to the composite columns with high levels of initial applied load. This may be due to the fact that when the initial load applied on columns is low, the degree of deterioration of the concrete's mechanical properties is high, since the exposure time of column to fire is higher. It is noticed that there is an extra difficulty in modelling the structural behaviour of concrete, especially in fire situations. Finally, (iii) the model developed in this study might have the potential to be used in developing parametric studies to obtain analytical formulae for simplified design or verification of the fire resistance of composite columns.

REFERENCES

ABAQUS. 2010. *ABAQUS/CAE Standard User's Manual, version 6.10-1*. Simulia Corp., USA.

Correia AJPM, Rodrigues JPC. 2011. Fire resistance of partially encased steel columns with restrained thermal elongation. *Journal of Constructional Steel Research* 67:593-601.

Ellobody E, Young B. 2010. Investigation of concrete encased steel composite columns at elevated temperatures. *Thin Walled Structures* 48:597-608.

EN 1991-1-2. 2002. *Basis of Design and Actions on Structures – Part 1-2: Actions on Structures Exposed to Fire.* European Community. CEN, Brussels.

EN 1993-1-2. 2004. *Eurocode 3: Design of steel structures, Part 1-2: General rules, Structural fire design.* European Committee for Standardisation, Brussels, Belgium.

EN 1994-1-1. 2003. *Eurocode 4 - Design of composite steel and concrete structures – Part 1-1: General – General rules and rules for buildings*. European Community. Brussels, Belgium.

EN 1994-1-2. 2005. *Eurocode 4 – Design of composite steel and concrete structures: Part 1.2: General rules Structural fire design*. CEN, Brussels.

Espinos A, Romero M, Hospitaler A. 2010. Advanced model for predicting the fire response of concrete filled tubular columns. *Journal of Constructional Steel Research* 66:1030-1046.

Huang Z, Tan K, Phng G. 2007a. Axial restraint effects on the fire resistance of composite columns encasing I-section steel. *Journal of Constructional Steel Research* 63:437–447.

Huang ZF, Tan KH. 2007b. Structural response of restrained steel columns at elevated temperatures. Part 2: FE simulation with focus on experimental secondary effects. *Engineering Structures* 29:2036-2047.

Huang Z, Tan K, Toh W, Phng G. 2008. Fire resistance of composite columns with embedded I-section steel - Effects of section size and load level. *Journal of Constructional Steel Research* 64:312–325.

Pires TAC, Rodrigues JPC, Silva JJR. 2012. Fire resistance of concrete filled circular hollow columns with restrained thermal elongation. *Journal of Construction Steel Research* 77:82-94.

Wang ZH, Tan KH. 2006. Residual Area method for heat transfer analysis of concrete-encased I-sections in fire. *Engineering Structures* 28:411-422.

TECHNICAL SHEET 5

NUMERICAL MODELLING OF CONCRETE-FILLED ELLIPTICAL HOLLOW SECTION COLUMNS AT AMBIENT TEMPERATURE

C. Fang, M. Theofanous and L. Gardner

(Imperial College London, United Kingdom)

NUMERICAL MODELLING OF CONCRETE-FILLED ELLIPTICAL HOLLOW SECTION COLUMNS AT AMBIENT TEMPERATURE

This work presents a numerical modelling strategy for predicting the compressive response of concrete-filled elliptical hollow section (EHS) stub columns at ambient temperature. Existing test data on such columns are presented first, and selected test specimens are employed to compare with the numerical models developed in this study. The general-purpose finite element software package ABAQUS is used to perform the numerical analysis. The influences of concrete model parameters, reinforcement, and element types on the axial response of the models are discussed. It is generally found that the failure mode and load-end shortening response of the considered columns are sensitive to the chosen type of concrete constitutive model. Both shell and solid elements can be suitable to discretize the steel tube, although a very small discrepancy between the two is found. In addition, reinforcement is shown to be able to increase the ultimate load.

1. INTRODUCTION

The application of concrete-filled tubular columns on modern building structures is considerably expanded nowadays due to their high load carrying capacity and sound ductility. In particular, the presence of the steel tube provides effective confinement on the concrete core, and thus increasing the concrete strength; concurrently, the presence of the concrete offers a constraining effect, which postpones the initiation of local buckling of the steel tube. The interaction effect between concrete and steel tube can lead to an improvement of the efficiency of material utilisation. The most commonly used cross-section types for such columns are circular, square, and rectangular shapes. Recently, a new class of cross-section type, namely, elliptical sections, have received great attention due to their combined aesthetics and structural efficiency with different major and minor axis properties. The availability of standard section profiles of EHS also encourages a wider usage of these sections.

This work focuses on numerical modelling of concrete-filled elliptical hollow section (CFEHS) stub columns. The cross-sectional compressive behaviour is mainly discussed, while global buckling is not considered in this study. A review of existing studies of CFEHS columns at ambient temperature is presented first in order to create a common database. The relevant studies include both experimental and numerical works. Selected tests are subsequently used to compare with the FE models developed in study, where the influences of concrete model parameters, reinforcement, and element types are discussed.

2. EXISTING WORK ON CFEHS COLUMNS

Yang et al. (2008) conducted 21 ambient tests to investigate the behaviour of stub CFEHS columns under axial compression. In the test programme, 9 test specimens were normally loaded (compositely loaded), 6 test specimens were loaded through the concrete core to investigate confinement effects, and the remaining 6 test specimens were normally loaded, but grease was applied prior to casting to simulate possible shrinkage of concrete. Three nominal tube thicknesses (4 mm, 5 mm and 6.3 mm) and three concrete grades

(C30, C60 and C100) were considered. Typical failure modes of the test specimens are shown in Fig. 1. The test results showed that the compressive response of CFEHS columns was sensitive to steel tube thickness and concrete strength, where a higher tube thickness could increase the load carrying capacity and enhance the ductility. In addition, increasing the concrete strength could improve the load-carrying capacity but reduce the ductility. The effect of concrete shrinkage was small, as indicated by the test result showing that the greased specimens and the normal ones had similar responses. For the case of the core-loaded specimens, both the confined concrete strength and ductility was found to be greatly improved over that of the unconfined concrete.

The design expressions from current European, North American, Japanese, British and Chinese Standards were also assessed by Yang et al. (2008). It was found that the existing design rules for concrete-filled SHS and RHS could be safely applied to CFEHS, and the EC4 design expression for concrete-filled SHS and RHS could provide an accurate prediction of the CFEHS behaviour. Following the experimental work done by Yang et al. (2008), numerical models using ABAQUS/Standard solver (ABAQUS 2010) were developed to simulate the tests (Dai & Lam 2010). Importantly, a new stress-stain curve was exclusively proposed for confined concrete in CFEHS. The proposed FE model was found to correlate well with the tests, particularly in terms of axial compressive resistance and deformation shape.

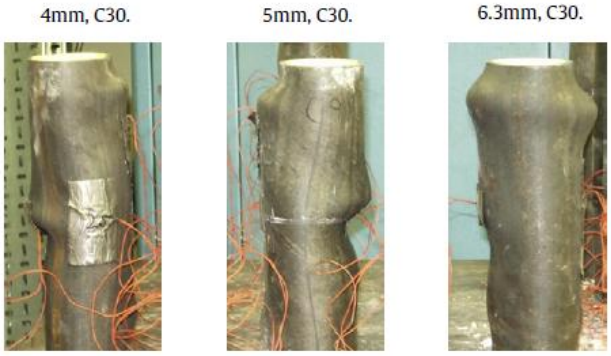

Fig. 1. Test specimens and FE models of CFEHS columns – Lam and colleagues.

An independent experimental research programme on stub CFEHS columns was conducted by Zhao & Packer (2009). Stub column tests on unfilled EHS were performed first, and the behaviour of CFEHS specimens were subsequently examined. For the CFEHS specimens, three loading cases were considered; i.e., loading through the whole cross-section, loading through concrete alone and loading through steel alone. Both normal concrete and self-consolidating concrete (SCC) were used in the test programme. One of the important findings from the tests was that very small concrete confinement at ultimate capacity of the stub column was observed. In view of this, it was suggested that a simple superposition of the steel strength and the concrete strength might give good predictions of the ultimate capacity of stub CFEHS columns. In addition, the load carrying capacity obtained from the test was compared with that predicted using EC4 and CAN/CSA-S16. The design rules in CSA-S16-01, CSA-S16-09 and EC4 for concrete-filled CHS were found to be applicable to CFEHS short columns, where the CHS diameter can be taken as an equivalent diameter when calculating the D/t and L/D ratios. For the CFEHS columns with only the concrete core loaded in axial compression, it was shown that very significant concrete confinement was generated. On the other hand, when

loaded through steel alone, the concrete was found to just affect the point of onset of local buckling by changing the local buckling mode.

Recently, Sheehan et al. (2012) examined the behaviour of short CFEHS columns under a combination of axial force and bending moment through both experimental and numerical studies. A total of 8 specimens were tested with two different tube wall thicknesses. The axial compression load was applied with various eccentricities. It was observed that the response of eccentrically loaded CFEHSs were sensitive to tube thickness, loading eccentricity and axis of bending. The tests were simulated using FE models, and the effect of different material constitutive models for concrete was studied. In order to achieve a good agreement between the test results and the FE predictions, the Dai & Lam (2010) model was recommended for the specimens with lower load eccentricities, the Han et al. (2007) model was suggested for those with higher eccentricities, and a combined concrete constitutive model falling in the middle of the two was recommended for those with intermediate load eccentricities. Subsequently, analytical interaction curves were generated and were compared with the experimental and FE results. The curves were shown to be efficient for the majority of non-slender cross-sections, but could be over-conservative for some stocky sections.

3. NUMERICAL MODELLING OF SELECTED TESTS

Six specimens from the tests conducted by Yang et al. (2008) are selected for the numerical modelling. The geometric properties and material properties for the six test specimens are listed in Table 1. All specimens were 300 mm long, and were uniaxially loaded with no eccentricity (e_y=e_z=0). General nonlinear finite element (FE) software package ABAQUS is used to simulate the selected test specimens. Eight-noded solid elements with reduced integration C3D8R are employed for discretizing both steel tube and concrete core, as shown in Fig. 2. The mesh sizes for the concrete and steel tube are 10 mm and 5 mm, respectively. Two rigid plates, which are 'tied' to the steel tube and 'hard contacted' to the concrete core, are placed at the top and bottom of the column. The bottom rigid plate is fixed by all six degrees of freedoms, while the top rigid plate is fixed by five degrees of freedoms, and only the axial displacement is allowed. A friction factor of 0.3 along the tangential directions of all 'hard contacts' is applied. To consider the confinement effect of concrete, a four-part stress-strain model proposed by Lam and co-workers is adopted. Details of the model can be found in Dai & Lam (2010). The Drucker-Prager model is adopted for concrete, and the following parameters are considered: flow potential eccentricity = 0.1, angle of friction = 25°, flow stress ratio = 0.8, and dilation angle = 15°. The stress-strain relationships for the steel tubes are based on the coupon test results. General static analysis with displacement control is conducted to obtain the load-end shortening responses of the column models.

Table 1. Geometric and material properties of selected specimens.

Specimens	2a (mm)	2b (mm)	t (mm)	E_s (Mpa)	f_y (MPa)	f_u (MPa)	$f_{ck,cube}$ (MPa)	f_{ck} (MPa)
150×75×4-C30	150.40	75.60	4.18	217500	376.5	513	36.9	30.5
150×75×5-C30	150.12	75.65	5.12	217100	369.0	505	36.9	30.5
150×75×6.3-C30	148.78	75.45	6.32	216500	400.5	512	36.9	30.5
150×75×4-C60	150.57	75.52	4.19	217500	376.5	513	59.8	55.3
150×75×5-C60	150.23	75.74	5.08	217100	369.0	505	59.8	55.3
150×75×6.3-C60	148.92	75.56	6.43	216500	400.5	512	59.8	55.3

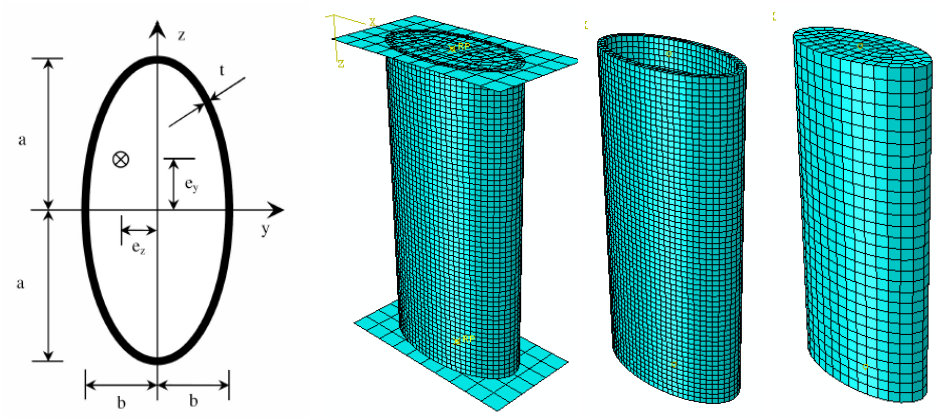

Fig. 2. FE model for selected test specimens

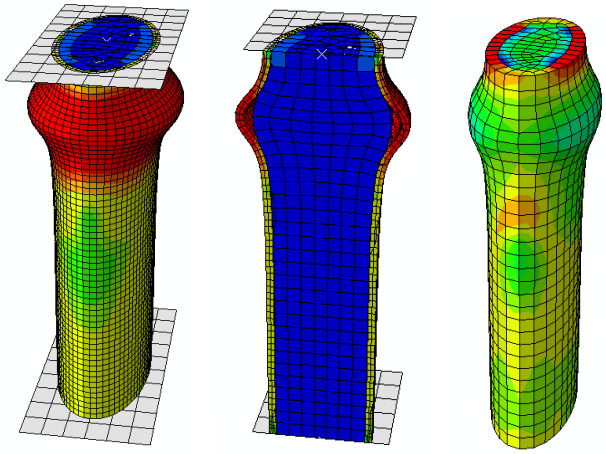

Fig. 3. Deformation of FE model.

Fig. 3 shows the typical deformation shape of the FE model under an axial column end shortening of 30 mm. An 'elephant foot' type of failure is generally observed. The load-end shortening responses obtained from the FE analysis and tests are shown in Fig. 4. Reasonable comparisons between the FE predictions and test results are generally observed, which indicates that the modelling strategy proposed in this study is reliable.

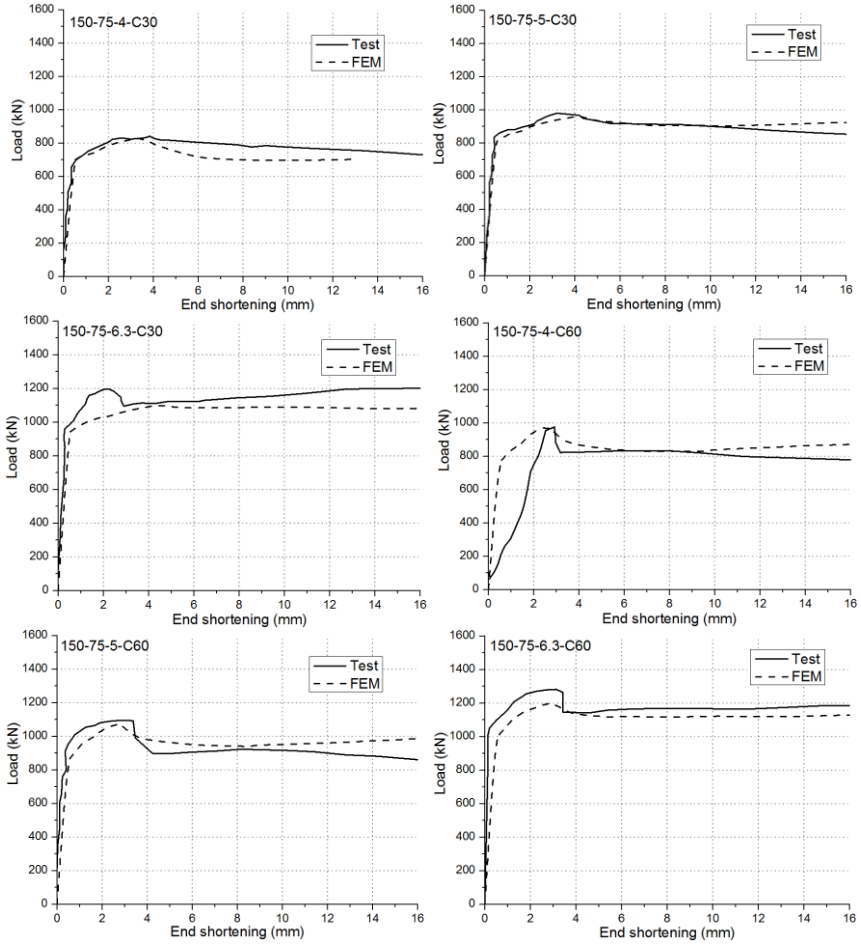

Fig. 4. Comparison of load-end shortening responses between FE analysis and test.

4. FURTHER DISCUSSIONS

4.1. INFLUENCE OF CONSTITUTIVE MODEL FOR CONCRETE

In this section, the Concrete Damage Plasticity (CDP) model, which is a modification of the Drucker–Prager strength hypothesis, is employed and compared with the Drucker-Prager model. The parameters adopted for the CDP constitutive model are listed in Table 2. The influences of dilation angle, f_{bo}/f_{co} (ratio of the strength in the biaxial state to the strength in the uniaxial state), and compressive damage are discussed.

Table 2. Parameters for Concrete Damage Plasticity concrete model.

Parameters	CDP1	CDP2	CDP3	CDP4	CDP5
Dilation angle (°)	15	0	15	15	0
Eccentricity	0.1	0.1	0.1	0.1	0.1
Biaxial/uniaxial f_{bo}/f_{co}	1.16	1.16	1.00	1.16	1.00
K value	0.667	0.667	0.667	0.667	0.667
Tensile stress (MPa)	2.8	2.8	2.8	2.8	2.8
Tensile Fracture Energy (N/m)	60	60	60	60	60
Compressive damage	-	-	-	enabled	enabled

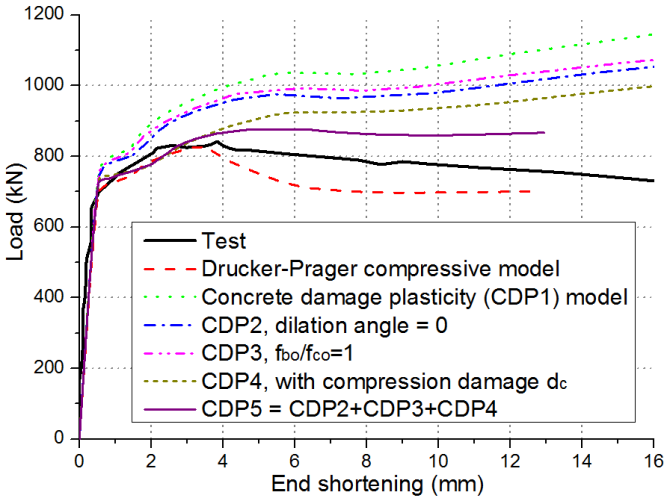

Fig. 5. Comparison of load-end shortening response with different concrete models.

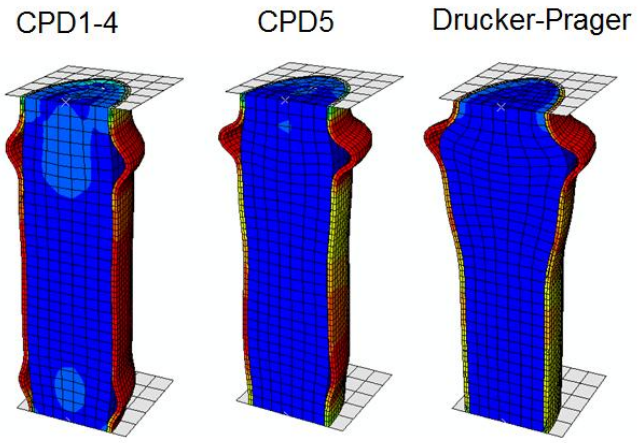

Fig. 6. Comparison of deformation shapes for different concrete models.

Fig. 5 shows the load-end shortening responses of the models with different concrete constitutive models. Only the models using the CDP5 and Drucker-Prager concrete models can achieve reasonable agreements compared with the test results. For those with CDP1 to CDP4, the load carrying capacity keeps increasing beyond the initial crush of concrete. Fig. 6 shows the deformation shape of the model, using the various concrete constitutive models, under an end-shortening of 30 mm. It is found that when CPD1 through CPD4 are employed, local buckling occurs near the top and bottom of the steel tube; for CDP5, where the dilation angle is taken as zero, and the f_{bo}/f_{co} ratio is taken as 1.0, the local buckling near the bottom of the column becomes less evident. When the Drucker-Prager model is employed, local buckling only occurs near the top of the column, and this is due to the quick decreasing of the concrete strength after initial concrete crushing, as confirmed in Fig. 5.

4.2. INFLUENCE OF ELEMENT TYPE FOR STEEL TUBE

In this section, the model using shell elements S4R for the discretization of the steel tube is compared with that using solid elements. S4R elements are general purpose elements with reduced integration, capable of capturing both thick and thin shell behaviour, and consisting of four nodes, with 6 degrees of freedom per node. The reference surface of the shell elements is considered to lie in the mid-thickness of the steel tube. The steel material model of the shell elements is identical to that previously used for the solid elements (Drucker-Prager model is used for the concrete core). The comparison is shown in Fig. 7. It is found that both modelling strategies for the steel tube are reasonably accurate. The discrepancy between the two models is limited.

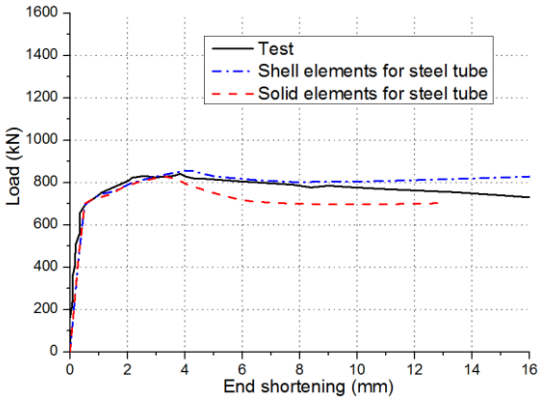

Fig. 7. Comparison of load-end shortening response with different element types for steel tube.

4.3. INFLUENCE OF REINFORCEMENT

The possible beneficial effect of reinforcement is considered. Truss elements are used for the reinforcement, as shown in Fig. 8. The nodes of the truss elements are assumed to be tied to the nodes of the surrounding concrete. The cross-sectional area of each bar is 100 mm^2, which makes a reinforcement ratio of approximately 5.3%. Loop bars are also considered in the model. It is shown that the deformation (expansion) of concrete is effectively constrained by the presence of the loop reinforcement. The load carry capacity is also evidently increased, as shown in Fig. 9. Further experimental studies are required to confirm this finding.

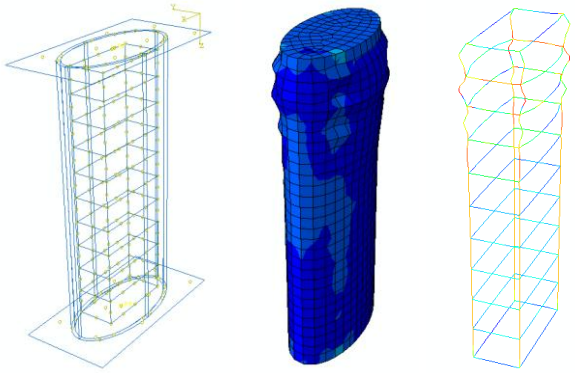

Fig. 8 Deformation of concrete and reinforcement.

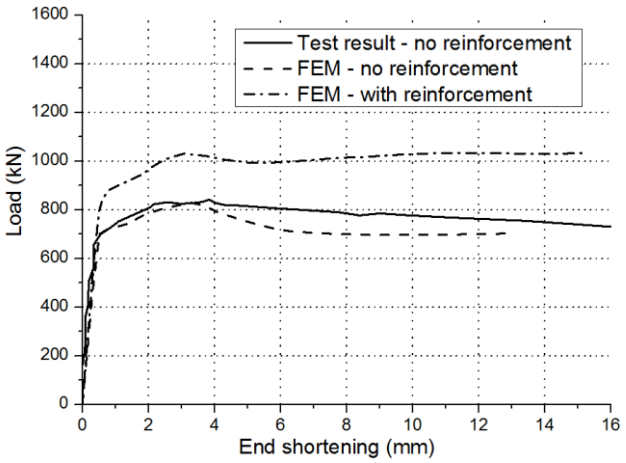

Fig. 9 Comparison of load-end shortening response with and without reinforcement.

5. CONCLUSIONS

This work presents numerical modelling strategies for concrete-filled elliptical hollow section (CFEHS) stub columns. The results may provide useful information for researcher and engineers for the effective modelling of such columns. It is generally found that: 1) the modelling strategies proposed by Dai & Lam (2010), employing the proposed concrete stress-strain relationship, can predict the behaviour of short concrete-filled EHS columns reasonably well; 2) the Drucker-Prager compressive model seems to be adequate for modelling the confined concrete in concrete-filled EHS columns, particularly for predicting the load-deformation response; 3) the concrete damaged plasticity model may be also feasible, provided that some input parameters are specifically defined, in particular, dilation angle=0, f_{bo}/f_{co}=0, and appropriate compression damage parameters should be included; 4) The difference between using solid and shell element for the steel tube is negligible for the 'pre-peak' behaviour, but a slight difference is found when predicting the 'post-peak' behaviour; and 5) the reinforcement is beneficial for improving the ultimate load capacity.

REFERENCES

ABAQUS. 2010. Version 6.10. Dassault Systemes Simulia Corp. Providence, RI, USA.

Dai X, Lam D. 2010. Numerical modelling of the axial compressive behaviour of short concrete-filled elliptical steel columns. *Journal of Constructional Steel Research* 66:931-942.

Sheehan T, Dai XH, Chan TM, Lam D. 2012. Structural response of concrete-filled elliptical steel hollow sections under eccentric compression. *Engineering Structures* 45:314-323.

Yang H, Lam D, Gardner L. 2008. Testing and analysis of concrete-filled elliptical hollow sections. *Engineering Structures* 30:3771-3781.

Zhao XL, Packer JA. 2009. Tests and design of concrete-filled elliptical hollow section stub columns. *Thin-Walled Structures* 47:617-628.

Project carried out with a financial grant of the Research Programme
of the Research Fund for Coal and Steel
(RFSR-CT_2012_00025)

Partners: